Accurate ab initio potential energy surface, rovibrational energy levels and resonance interactions of triplet (x3B1) methylene

Oleg Egorov, Michael M. Rey, Dominika Viglaska, Andrei Nikitin

Accurate *ab initio* potential energy surface, rovibrational energy levels and resonance interactions of triplet ($\widetilde{X}^3B_1$) methylene

Oleg Egorov[1,2*], Michaël Rey[3], Dominika Viglaska[3], Andrei V. Nikitin[1,2]

[1]Laboratory of Theoretical Spectroscopy, V.E. Zuev Institute of Atmospheric Optics SB RAS 1, Akademician Zuev Sq., Tomsk, 634055 Russia

[2]Faculty of Physics, Tomsk State University 36, Lenin Ave., Tomsk, 634050 Russia

[3]Groupe de Spectrométrie Moléculaire et Atmosphérique UMR CNRS 7331, UFR Sciences BP 1039, 51687 Reims Cedex 2, France

Corresponding Author

*(O.E.) E-mail: oleg.egorov@iao.ru

ABSTRACT

In this work, we report rovibrational energy levels for four isotopologues of methylene (CH_2, CHD, CD_2, and $^{13}CH_2$) in their ground triplet electronic state ($\tilde{X}^3B_1$) from variational calculation up to ~10000 cm^{-1} and using a new accurate *ab initio* potential energy surface (PES). Triplet methylene exhibits a large-amplitude bending vibration and can reach a quasilinear configuration due to its low barrier (~2000 cm^{-1}). To construct the *ab initio* PES, the Dunning's augmented correlation-consistent core-valence orbital basis sets were employed up to the sextuple-ζ quality [aug-cc-pCVXZ, X=T, Q, 5, and 6] combined with the single- and double-excitation unrestricted coupled cluster approach with a perturbative treatment of triple excitations [RHF-UCCSD(T)]. We have shown that the accuracy of the *ab initio* energies is further improved by including the corrections due to the scalar relativistic effects, DBOC and high-order electronic correlations. For the first time, all the available experimental rovibrational transitions were reproduced with errors less than 0.12 cm^{-1}, without any empirical corrections. Unlike more "traditional" nonlinear triatomic molecules, we have shown that even the energies of the ground vibrational state (000) with rather small rotational quantum numbers are strongly affected by the very pronounced rovibrational resonance interactions. Accordingly, the polyad structure of the vibrational levels of CH_2 and CD_2 was analyzed and discussed. The comparison between the energy levels obtained from the effective Watson *A*-reduced Hamiltonian, from the generating-function approach and from a variational calculation was given.

Keywords: CH_2, triplet methylene, *ab initio*, rovibrational levels, large-amplitude motion, centrifugal distortion, resonance interactions

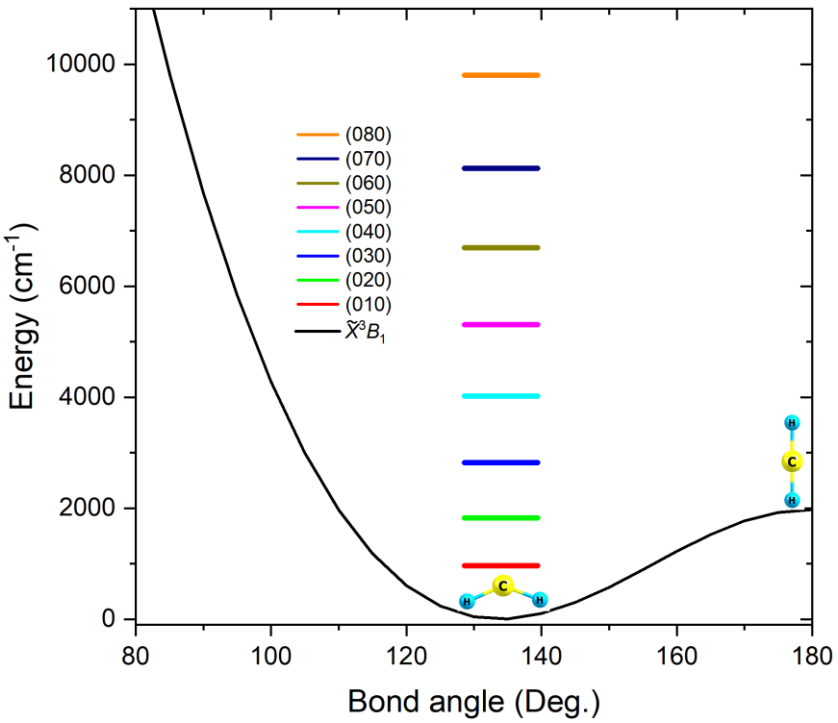

Graphical Abstract

Overtones of the bending mode of triplet methylene predicted from the developed ab initio PES

1. INTRODUCTION

Methylene (CH_2) is a simple hydrocarbon radical with a complicated rovibrational structure in its ground triplet electronic state ($\tilde{X}^3B_1$, hereafter denoted as $\tilde{X}$) due to the low barrier to linearity (~2000 cm^{-1}) and the anomalous centrifugal distortion. Triplet methylene [$CH_2(\tilde{X})$] was the subject of many works, mainly devoted to the rovibronic spectra within the ground and first excited vibrational states. Fundamental stretching bands, overtones and combination bands were not assigned from high-resolution spectra so far. This is partly explained by the presence of the low-lying excited singlet state ($\tilde{a}^1A_1$, hereafter denoted by $\tilde{a}$) which is responsible for the strongest absorption above 3000 cm^{-1}. Moreover, the extremely short lifetime of CH_2 due to its high reactivity makes the spectra analysis very difficult.

Since CH_2 is one of the primary products involved in the methane photolysis (see *e.g.* Blitz *et al.*[1]), it is likely that it exists in methane-rich planetary atmospheres and in the interstellar medium. According to Gans *et al.*,[2] the quantum yields of CH_2 are comparable with that of the methyl radical (CH_3) while the amount of $CH_2(\tilde{X})$ and $CH_2(\tilde{a})$ strongly depends on the excitation wavelength. If the wavelength differs from the Lyman-α line at 121.6 nm, then it can lead to the formation of both CH_3 and $CH_2(\tilde{X})$. An additional formation channel of $CH_2(\tilde{X})$ can be due to the inelastic collisions of $CH_2(\tilde{a})$ with atmospheric species. The rate coefficients measured by Douglas *et al.*[3] demonstrated a dominance of the relaxation to the ground electronic state when the temperature is below 100 K.

At the present time, $CH_2(\tilde{X})$ was observed in the interstellar medium near the Orion-KL and the W51 M sources by Hollis *et al.*,[4] and near molecular cloud complexes Sagittarius B2 and W49 N by Polehampton *et al.*[5] In both cases, the unambiguous detection became possible with the help of accurate spectroscopic data for which fine and hyperfine structures were measured for several pure rotational transitions of $CH_2(\tilde{X})$ (see *e.g.* Lovas *et al.*,[6] Michael *et al.*,[7] and Brünken *et al.*[8,9]).

This work was motivated by the following two reasons.

1. No accurate *ab initio* potential energy surfaces (PES) of $CH_2(\tilde{X})$ constructed from high-level orbital basis sets and including corrections such as the diagonal Born-Oppenheimer correction (DBOC), scalar relativistic effects and high-order electronic correlations were available so far. The most recent theoretical calculations to date using the aug-cc-pCVQZ basis set were performed by Furtenbacher *et al.*[10] Their band origin for the bending band ν_2 was predicted with an error of 4 cm^{-1}, which is generally not enough for atmospheric applications. According to the recent paper by Coudert,[11] the global fit of the $CH_2(\tilde{X})$ transitions is not unambiguous and "…*a more accurate potential energy surface is needed to understand the nature of these discrepancies*…".

2. No accurate variationally-computed highly-excited energy levels of $CH_2(\tilde{X})$ were available so far, though they are required to construct comprehensive line lists. In a series of papers by Bunker

and Jensen,[12–15] the perturbation-based approach ("Nonrigid bender Hamiltonian") as well as the kinetic energy operator implemented in the MORBID computer code of Jensen[16] were employed, together with empirically-refined PESs. However, as it was demonstrated previously by Barclay *et al.*,[17] the truncated kinetic energy operator involved in MORBID may introduce errors of several wavenumbers during energy levels calculation of quasilinear molecules such as $CH_2(\tilde{X})$.

Currently, accuracy of the rovibrational transitions is typically within a wavenumber using the best available high level *ab initio* methods.[18, 19] One of the advantages of using *ab initio* PESs in conjunction with variational calculations is that all vibrational degrees of freedom are properly taken into account. In the effective approach, only a small set of interacting vibrational states is generally studied and beyond the range of observed data the extrapolation power is often limited. Consequently, performing variational calculations is more suitable for $CH_2(\tilde{X})$ because of the lack of experimental data for high energy levels. Császár *et al.*[20] demonstrated that the band origin of ν_2 can be predicted with an error of 1.5 cm^{-1}. In this work, we have shown that such accuracy can be improved by a factor 20. Moreover, we focused not only on the fundamental bands but also on the simultaneous calculation of all vibrational bands up to ~10000 cm^{-1} for the four isotopologues CH_2, CHD, CD_2, and $^{13}CH_2$. To this end, a new accurate *ab initio* PES will be presented in this paper.

The article is organized as follows. In the next Section 2 the state-of-the-art in the spectroscopy of triplet methylene will be given. Section 3 will present the *ab initio* methods used in the present work and give the analytical form of the PES allowing a good description of both the equilibrium geometry and height of the barrier to linearity. The nuclear-motion Hamiltonian described in Ref. 21 will be also briefly discussed. In Section 4, the calculated rovibrational energy levels will be compared to both available experimental data and previous *ab initio* results. Unusual resonances and centrifugal distortions will be discussed before concluding.

To perform *ab initio* calculations, the MOLPRO,[22, 23] MRCC,[24, 25] and CFOUR[26, 27] packages were used. The nuclear motion calculations were carried out using our home-made variational computer code TENSOR[28–30] applied with success in Refs. 31–43 for computing accurate rovibrational energy levels and line intensities of different polyatomic semirigid and nonrigid molecules.

2. SPECTROSCOPY OF $CH_2(\tilde{X})$: STATE-OF-THE-ART

2.1. Experimental studies

First successful spectroscopic studies of CH_2 were done by Herzberg *et al.*[44–46] by the flash photolysis of diazomethane (CH_2N_2) in the presence of the inert gas N_2. Several experiments were carried out with deuterated diazomethane. Two band systems belonging to CH_2 were thus located: one in the ultraviolet region (at 141.5 nm) and another one in the red region at 819, 731.5, and 653.1

nm. The spectral structures of the ultraviolet band suggested that CH_2 had to be close to the linear configuration in its ground triplet electronic state while the observed ΔK series in the red region were typical for a bent singlet configuration. Since the intensity of the ultraviolet band increases with the concentration of the inert gas, more collisions were needed to reach the triplet state which probably corresponds to the "true" ground electronic state of CH_2, although the energy difference between the two lower states was not accurately determined.

Further theoretical and experimental works allowed to determine how much $CH_2(\tilde{X})$ deviates from linearity. According to the electron paramagnetic resonance spectra measured by Bernheim *et al.*[47, 48] and Wasserman *et al.*,[49–52] $CH_2(\tilde{X})$ has a strongly bent configuration with an angle around 130°–140°. This was confirmed from *ab initio* calculations performed by Harrison *et al.*,[53, 54] Bender *et al.*,[55, 57] O'Neil *et al.*,[58] and Hay *et al.*[59] The anomalously large values of the rotational constants were corroborated by the ultraviolet spectrum at 141.5 nm observed by Herzberg *et al.*[44–46] The missing transitions for $K>0$ can be explained by the predissociation properties of the upper electronic state, as discussed in Ref. 60.

First observation of pure rotational transitions of $CH_2(\tilde{X})$ was reported by Mucha *et al.*[61] using the laser magnetic resonance (LMR) spectroscopy technique. High-resolution spectra were then systematically studied by Sears, McKellar *et al.* using both the LMR[62–65] and diode laser spectroscopy.[66–68] Fine and hyperfine structures for the pure rotational and fundamental vibrational bands were then characterized while the fit of molecular effective parameters for the (000) and (010) vibrational states allowed to obtain an accurate equilibrium geometry of $CH_2(\tilde{X})$ as well as the band center of ν_2. These values were also obtained for $CD_2(\tilde{X})$[66, 69, 70] and $^{13}CH_2(\tilde{X})$.[71]

In addition, McKellar *et al.*[65] measured the rotational transitions for the ground vibrational state of $CH_2(\tilde{a})$ as well as some allowed singlet-triplet transitions due to the non-zero values of the spin-orbital coupling (SOC) matrix elements. The energy difference (in terms of the T_0 and T_e parameters) between the triplet and singlet states – the so called singlet-triplet splitting – turned out to be more precise than previous *ab initio* calculations[54, 59, 72–83] and experimental results.[84–93] Note that the interpretation of the high-resolution spectra was made possible using the *ab initio* fine structure parameters and SOC matrix elements calculated by Langhoff *et al*.[94–96]

The ground electronic state of methylene was also studied from photoelectron spectra of the methylene anions (CH_2^- or CD_2^-) by Sears and Bunker,[97, 98] by Leopold *et al.*,[99] and more recently by Coudert *et al.*[100] The frequencies of the bending overtones up to $\upsilon_2 = 7$ were reported in Ref. 99 with an accuracy of ~30-40 cm^{-1}. In a series of papers by Petek *et al.*[101–104] devoted to the study of rovibrational spectra for the singlet $CH_2(\tilde{a})$ methylene, the manifestation of perturbation on the energy levels of both singlet and triplet methylene, caused by the singlet-triplet coupling, was analyzed.

2.2. Theoretical description

A new set of experimental data led to a series of works by Bunker and Jensen devoted to the construction of an accurate empirical PES for $CH_2(\tilde{X})$. In early works,[12] the parameters of the nonrigid bender Hamiltonian[105–107] were fitted to experimental transitions. In this Hamiltonian, the kinetic energy part is based on the Hougen-Bunker-Johns (HBJ) formalism[108] where the expansion parameters of the reciprocal $\mu_{\alpha\beta}$ tensor ($\mu_{\alpha\beta}$ is the inverse of $I'_{\alpha\beta}$ which is related to the inertia matrix $I_{\alpha\beta}$ in accordance with Eq. (4.8) of Ref. 109) depend explicitly on the bending angle while the effects of the centrifugal distortion and anharmonicity coming from the stretching vibrations are treated using Van Vleck perturbation theory. This model allowed to characterize observed rovibrational transitions of $CH_2(\tilde{X})$, $CD_2(\tilde{X})$, and $^{13}CH_2(\tilde{X})$ and to determine the empirical values of the equilibrium geometry as well as the height of the barrier to linearity from fitted PES parameters. In order to treat the singularity, perturbation theory was improved in Refs. 109–111 by including in the energy denominators of the perturbation series the dependence on the bending vibration quantum number (υ_2) and on the rotational quantum number (K). This led to two versions of the nonrigid bender Hamiltonian (called "NRB1" and "NRB2") given in Ref. 14 with quite close results obtained by data fitting but with rather different energy levels for the stretching modes for which experimental information was missing.

A first variational calculation for $CH_2(\tilde{X})$ was presented in Ref. 15 using the MORBID Hamiltonian developed by Jensen.[16] Unlike the nonrigid bender Hamiltonian, all available experimental data were included into the fit, particularly those associated with the rotational transitions within the (100) stretching state. Almost at the same time, McLean *et al.*[112] and Comeau *et al.*[113] published one of the first pure *ab initio* PESs of $CH_2(\tilde{X})$ that were then applied to calculate its rovibrational energy levels. According to Barclay *et al.*,[17] the error on the energy levels between MORBID and Discrete Variable Representation (DVR) calculations is of several wavenumbers. Kozin *et al.*[114] implemented the spin-spin and spin-rotational terms in the MORBID computer code for fine structure calculations. The corresponding parameters were directly determined by data fitting.

High-level *ab initio* calculations of enthalpy of the $CH_2(\tilde{X})$ formation were carried out by Császár *et al.*[20] and Tajti *et al.*[115] The corrections due to the high-order electronic correlations, DBOC and relativistic effects were included. As already mentioned above, the excited energy levels of $CH_2(\tilde{X})$ were not studied in Ref. 20. Soon after, Furtenbacher et al.[10] performed DVR calculations for $CH_2(\tilde{X})$ with a deviation of 4 cm^{-1} for ν_2 while accuracy of their rovibrational transitions varied from 0.2 to 4.5 cm^{-1}. Again, only the fundamental bands were considered in Ref. 10. At the same time, a global *ab initio* PES was constructed by Medvedev *et al.*[116] in order to describe the chemical reaction

between the $CH_2(\tilde{X})$ and $CH_3(\tilde{X}^2A_2'')$ radicals. The difference between the calculated vibrational levels in the H + $CH_2(\tilde{X})$ dissociation channel using this global PES and those predicted from the empirically refined PES by Jensen *et al*.[15] was of a few tenths of wavenumbers.

2.3. Fine and hyperfine structures

Last but not least, an important aspect of the $CH_2(\tilde{X})$ spectroscopy concerns its hyperfine structure. Since the two hydrogen atoms of $CH_2(\tilde{X})$ have nonzero nuclear spin, $I(H_1) = I(H_2) = 1/2$, *para* ($I_{total} = 0$) and *ortho* ($I_{total} = 1$) configurations are possible. In the case of *ortho*-$CH_2(\tilde{X})$, each fine energy level further splits into three hyperfine sublevels. Lovas *et al*.[6] resolved the hyperfine splitting in the pure rotational transitions without using an external magnetic field (zero-field splitting). The information on the hyperfine splitting made it possible the unambiguous identification of methylene in the interstellar medium near the Orion-KL and the W51 M sources by Hollis *et al*.[4] New measurements with resolved fine and hyperfine structures by Ozeki *et al.*,[117, 118] Michael *et al.*,[7] and Brünken *et al*.[8, 9] extended the spectral region to lower frequencies, which are more suitable for cold observations of dense interstellar clouds. Polehampton *et al*.[5] used these new data to detect *ortho*- and *para*-$CH_2(\tilde{X})$ in the emission spectra toward the molecular cloud complexes Sagittarius B2 and W49 N. For the less studied deuterated isotopologue $CHD(\tilde{X}^3A'')$, several pure rotational transitions were measured by Nolte *et al.*[119] using the LMR spectroscopy and by Ozeki *et al.*[120] in field-free conditions.

3.4. Anomalous centrifugal distortion effects

The experimental transitions of $CH_2(\tilde{X})$ were generally fitted by using Watson *A*-reduced Hamiltonians and including spin-spin, spin-rotational, and electron-spin–nuclear-spin coupling terms. However, the centrifugal distortion terms are anomalously large, even for transitions with small values of the rotational quantum numbers. To improve the convergence of the Hamiltonian, the Euler expansion of the Hamiltonian was applied by Brünken *et al.*,[9] both for the rotational and spin-rotational parts. Recently, Coudert[11] performed a global fit of all transitions involved in the ground and first excited vibrational states. To this end, a modified version of the "Bending-Rotation" approach was used, assuming the dependence of the fine coupling terms on the large-amplitude bending coordinate (for further details, see Ref. 11 and references therein).

As it will be also shown, the ground vibrational state (000) of $CH_2(\tilde{X})$ is no longer isolated for $K_a \geq 5$ values. In that case, fitting $CH_2(\tilde{X})$ transitions using standard effective Hamiltonians is a tricky task because of strong rovibrational resonance interactions. Performing a variational calculation is thus fully justified in the present work.

3. METHOD

3.1. *Ab initio* calculations

Since the electronic structure of $CH_2(\tilde{X})$ is dominated by one electronic configuration, the single reference approach can be used to compute accurately the potential. For this reason, the spin-unrestricted coupled cluster (CC) method [RHF-UCCSD(T)] implemented in MOLPRO by Knowles *et al.* [121, 122] was employed. The validity of the CC method was confirmed by the T1 and D1 diagnostic numbers extracted from the output files of MOLPRO. These numbers depend on the amplitudes of the excitations and are used to estimate the multi-reference character of the problem. For all the nuclear configurations of our grid, the maximum values of T1 and D1 were about two times less than their critical values of 0.02 and 0.05, respectively, established by Lee *et al.*[123] and Janssen *et al.*[124]

The ground electronic state of methylene has different multiplicity and symmetry (under the C_s point group) compared to the first excited singlet state. This allows to explicitly distinguish these two electronic states during *ab initio* calculations. In this work, we do not consider the singlet-triplet transitions caused by the nonzero SOC matrix elements and do not focus on fine and hyperfine structures of the rovibrational levels of $CH_2(\tilde{X})$. Indeed, the spin-spin and spin-rotational parameters allowing an accurate description of the fine structure can be easily obtained by direct data fitting (see *e.g.* Ref. 114). Instead, the present study aims at computing an accurate PES for $CH_2(\tilde{X})$ and performing nuclear-motion calculations.

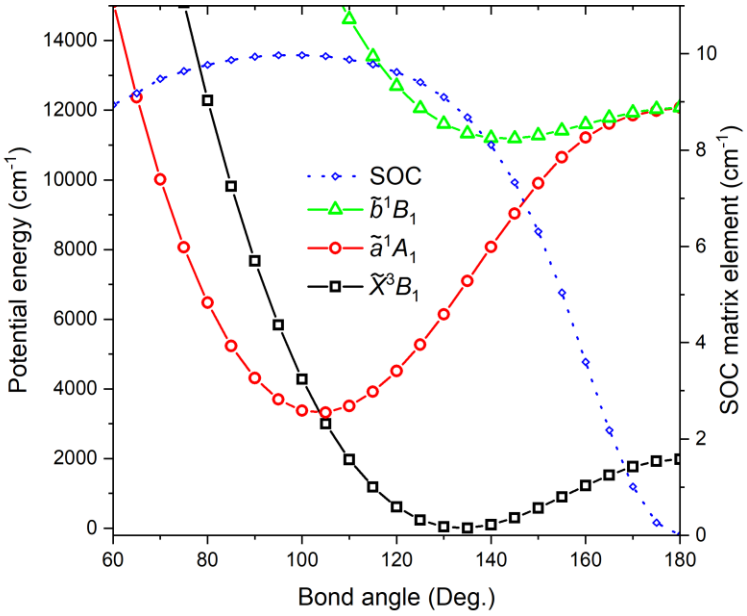

FIGURE 1 Plot of the 1D cuts for the three lowest electronic states of CH_2 calculated at the fixed bond length of r_1(C-H$_1$) = r_2(C-H$_2$) = 1.076 Ang. The blue curve corresponds to the biggest SOC matrix element between the ground triplet and first excited singlet states

Contrary to the energy levels of the ground electronic triplet state, the excited levels of the singlet methylene $CH_2(\tilde{a})$ are strongly perturbed by a Renner-Teller effect, caused by the degeneracy of $\tilde{a}$ and of the second excited singlet state ($\tilde{b}^1B_1$, hereafter $\tilde{b}$) at the linear configuration. Since the $\tilde{b}$ state has a rather shallow minimum of potential (less than 1000 cm^{-1}) with a quasilinear equilibrium bond angle of ≈143° (versus 102° for the $\tilde{a}$ state), the strong manifestation of the Renner-Teller effect occurs only for levels with $\upsilon_2 \geq 4$ for $CH_2(\tilde{a})$. For further details on the Renner-Teller effect, the reader can refer to the corresponding theoretical and experimental works by Duxbury *et al.*,[125] Alijah *et al.*,[126] Green *et al.*,[127] Xie *et al.*,[128] Hartland *et al.*,[129] and Gu *et al.*[130]

In order to show the structure of the three lowest electronic states of CH_2, the 1D cuts calculated at the icMRCI(Q)/aug-cc-pCVQZ level of the theory using the state-average CASSCF(8, 5) are displayed in **Figure 1**. The blue curve in **Figure 1** describes the angular dependence of the largest SOC matrix element responsible for the singlet-triplet transitions. As it can be seen, the maximum value of SOC is not big (≈10 cm^{-1}), compared to the potential energies, and equals zero at the linear configuration. Accordingly, the effect of SOC is mainly determined by the *diagonal* elements of the spin-orbit matrix. For example, at r_1(C-H_1)=r_2(C-H_2)=1.076 Ang. the potential curves for the $\tilde{X}$ and $\tilde{a}$ states cross at the bond angle of 103–104°. The direct diagonalization of the spin-orbit matrix in MOLPRO led to the following shifts in the potential energies of the $\tilde{X}$ state: 1.16 and –2.5 cm^{-1} at 103° and 104°, respectively. Out of this region, the absolute shift was of 0.05 cm^{-1} in average, with a shift of 0.02 cm^{-1} at the bottom of the $\tilde{X}$ curve. Note that the description of the singlet-triplet transitions would require the evaluation of the spin-orbit matrix which is beyond the scope of the present work.

To analyze the convergence of the potential energies using the RHF-UCCSD(T) method, the Dunning's augmented correlation-consistent core-valence orbital basis sets[131] were applied up to the sextuple-ζ quality [aug-cc-pCVXZ, hereafter denoted as ACVXZ, where X=T, Q, 5, and 6] and all electrons were correlated (valence-valence, core-valence, and core-core contributions were included). Although the *ab initio* energies could be further extrapolated to the Complete Basis Set (CBS) limit using different extrapolation formula (see *e.g.* Ref. 132), our results prove that the ACV6Z basis set is enough to get a Root Mean Square (RMS) deviation better than 0.1 cm^{-1} for the band origins and better than 0.12 cm^{-1} for the rovibrational transitions.

In addition, we have tested the simplified explicitly correlated methods [RHF-UCCSD(T)-F12x{x=a, b}] of Knizia *et al.*[133] available in MOLPRO. The explicitly correlated methods can approach the CBS limit with less computational effort and is thus very relevant for polyatomic molecules with many electrons where the application of the "standard" CC method is difficult. Here, the benchmark calculation for the F12a,b methods was carried out using the correlation-consistent core-valence cc-pCVQZ-F12 basis set (hereafter, CVQZ-F12). For the specially optimized

correlation-consistent F12 basis sets, the appropriate defaults options are automatically chosen by MOLPRO (see Section 22.6 of the manual book[23]). Particularly, the suitable density fitting (DF) and resolution of the identity (RI) basis sets were automatically chosen as VQZ-F12/JKFIT and CVQZ-F12/OPTRI, respectively. The default Slater exponents were used for valence-valence, core-valence, and core-core pairs (GEM_BETA = [1, 1, 1]). The contribution of core orbitals to the singles energy was not included (CORE_SINGLES = 0) whereas the associated complementary auxiliary basis set (CABS) singles correction to the reference energy was taken into account (CABS_SINGLES=1).

We have shown that accuracy of the potential energies could be significantly improved by including corrections due to (i) scalar relativistic effects, (ii) DBOC as well as (iii) contributions to the correlation energy from highly-excited Slater determinants.

(i) The relativistic correction was obtained by calculating the RHF-UCCSD(T)/ACVQZ-DK energies from the Douglas-Kroll-Hess (DKH) scalar relativistic Hamiltonian expanded up to the fourth order. Higher-order transformations provide contributions that are less than 10^{-6} cm^{-1}. The energy difference, namely [RHF-UCCSD(T)+DKH/ACVQZ-DK] – [RHF-UCCSD(T)/ACVQZ], was then computed and added to the PESs.

(ii) The DBOC was calculated at the UHF-CCSD/cc-pVTZ level of the theory using the CFOUR computer code. It turns out that the CCSD approach is enough for most molecules, including CH_2, as it was already demonstrated by Gauss *et al.*[134] By default, CFOUR operates with nuclear masses for the main isotopologue. According to our estimations, if the nuclear masses of CD_2 are applied instead of those of $^{12}CH_2$ then the difference between the observed and calculated band center for ν_2 changes from 0.07 cm^{-1} to –0.09 cm^{-1}, which remains rather small in absolute value. It is also likely that the isotopic dependent DBOC allows a better agreement with observation for higher energies but it was not possible to check due to the absence of experimental data. Finally, we decided to construct one PES for all the isotopologues by including the DBOC contribution coming from $^{12}CH_2$.

(iii) One of the advantages of using the single reference CC method is that the accuracy of the correlation energy can be substantially improved by including contributions from high-order excitations. Since the number of the excited Slater determinants grows rapidly as the excitation order increases, the calculations become more and more time-demanding. However, in order to make calculations tractable, the high-order CC methods can be combined with less costly basis sets because they converge more rapidly with respect to the basis set size (see *e.g.* Ref. 135). For example, the total number of determinants for the biggest ACV6Z basis set is of 3084335 when the CC method restricted to single and double excitations [CCSD] is used. A similar number (2955831) is obtained after

including the contributions from the triple excitations [CCSDT], combined with the cc-pVQZ basis set. For the quadruple CC calculations [CCSDTQ], this number becomes two times bigger (6046929), even when the cc-pVTZ basis set is considered. Finally, the following basis sets were used in the MRCC code when making scaling from CCSD(T) to CCSDTQP: [CCSDT–CCSD(T)]/cc-pVQZ, [CCSDT(Q)–CCSDT]/cc-pVQZ, [CCSDTQ–CCSDT(Q)]/cc-pVTZ, and [CCSDTQP–CCSDTQ]/cc-pVDZ.

Finally, all the *ab initio* calculations presented here have been performed on the whole grid of the nuclear configurations (see next subsection) with a global energy threshold of 10^{-10} Hartree. The computed *ab initio* energies can be found in **Supplementary materials**.

3.2. Description of the PES

For energy calculations, the following three internal coordinates can be used in MOLPRO for $CH_2(\tilde{X})$: two bond lengths, r_1(C-H_1) and r_2(C-H_2), and one bond angle, α(H_1–C–H_2). However, the grid of points in this coordinate system was generated using symmetry coordinates transforming as the A_1 and B_2 irreducible representations of the C_{2v} point group, allowing smoother variations for the three internal coordinates. The symmetry coordinates are given by

$$\begin{cases} s_1^{A_1} = \left(\Delta r_1 + \Delta r_2\right)/\sqrt{2} \\ s_2^{A_1} = \Delta\alpha \\ s_3^{B_2} = \left(\Delta r_1 - \Delta r_2\right)/\sqrt{2} \end{cases} \quad (1)$$

where "Δ" means the deviation from the equilibrium values r_e and α_e, respectively.

Our grid of nuclear configurations consists of 1150 points with an energy range going from 0 to 15000 cm^{-1}. A special attention was made for the evaluation of the barrier to linearity: the bond angle was gradually scanned from 76° to 180° by step of 2° around its equilibrium value of ≈134° and for each value of α, $s_1^{A_1}$ and $s_3^{B_2}$ varied simultaneously. In particular, our grid consists of 84 different values of r_1 and r_2 at α = 180°, which is enough to determine accurately the equilibrium bond length at the linear configuration (hereafter, r_{linear}) as well as the barrier to linearity (hereafter, $E_{barrier}$).

Following our recent studies,[41, 42] the PES of $CH_2(\tilde{X})$ was expressed as a Taylor power series expansion in terms of the symmetry coordinates

$$V\left(S_1^{A_1}, S_2^{A_1}, S_3^{B_2}\right) = \sum_{i,j,k} C_{ijk} \cdot \left[S_1^{A_1}\right]^i \cdot \left[S_2^{A_1}\right]^j \cdot \left[S_3^{B_2}\right]^{2k}, \quad (2)$$

where C_{ijk} are expansion coefficient to be determined from the fit of the *ab initio* potential energies. The even powers for $S_3^{B_2}$ ensure that the potential transforms as the totally symmetric irreducible representation A_1. Following the MORBID approach,[16] Morse-cosine coordinates were preferred instead of (1) to define the symmetry coordinates in Eq. (2),

$$\begin{cases} S_1^{A_1} = (y_1 + y_2)/\sqrt{2} \\ S_2^{A_1} = a \\ S_3^{B_2} = (y_1 - y_2)/\sqrt{2} \end{cases}, \quad (3)$$

where y_1, y_2, and a are asymptotic functions depending on the internal coordinates as follows:

$$\begin{cases} y_1 = 1 - \exp\left[-b \cdot (r_1 - r_e)\right] \\ y_2 = 1 - \exp\left[-b \cdot (r_2 - r_e)\right], \\ a = \cos(\alpha) - \cos(\alpha_e) \end{cases} \quad (4)$$

where b = 1.5 Å^{-1}. It is also worth mentioning that the supplement angle $\bar{\rho} = 180^o - \alpha$ is introduced in the HBJ formalism to describe the potential energy function, while an "effective" coordinate ρ is introduced in the kinetic energy operator. It was shown that $\bar{\rho}$ and ρ can be related a through coordinate transformation.[109, 136]

TABLE 1 Impact of the basis set size on the structural parameters of the $CH_2(\tilde{X})$ PES at the RHF-UCCSD(T) level of the theory

Basis set	r_e (Ang.)	α_e (Deg.)	r_{linear} (Ang.)	$E_{barrier}$ (cm^{-1})	E_0(Hartree)
ACVTZ	1.077818	133.74601	1.067323	1981.511	–39.1301794830
ACVQZ	1.075978	133.84392	1.065630	1947.313	–39.1423138808
ACV5Z	1.075417	133.86762	1.065073	1937.292	–39.1457118077
ACV6Z	1.075300	133.88001	1.064952	1933.144	–39.1469010781
CVQZ-F12b	1.075216	133.87635	1.064844	1935.930	–39.1471016435
CVQZ-F12a	1.075190	133.92376	1.064870	1919.419	–39.1487912991

Notes:
All these values were determined from a fit of the *ab initio* PES.
E_0 is the total energy (Hartree-Fock + correlation) taken at the bottom of the PES, in Hartree.

TABLE 2 Contributions of the corrections to the equilibrium geometry and to the height of the barrier to linearity of $CH_2(\tilde{X})$

Ab initio level	r_e (Ang.)	α_e (Deg.)	r_{linear} (Ang.)	$E_{barrier}$ (cm^{-1})
RHF-UCCSD(T)/ACV6Z	1.075300	133.88001	1.064952	1933.144
+Relativistic/ACVQZ-DK	1.075187	133.88167	1.064805	1934.300 (+1.156)
+DBOC/VTZ	1.075332	133.90224	1.064933	1933.431 (–0.869)
+CCSDT/VQZ	1.075582	133.91237	1.065180	1928.319 (–5.112)
+CCSDT(Q)/VQZ	1.075649	133.92160	1.065262	1924.969 (–3.350)
+CCSDTQ/VTZ	1.075656	133.92230	1.065270	1924.690 (–0.279)
+CCSDTQP/VDZ	1.075660	133.92256	1.065274	1924.592 (–0.098)

Notes:
The *ab initio* value of the barrier lies between the two last Bunker and Jensen's results: 1931±30 cm^{-1} and 1916 cm^{-1} taken from Refs. 14 and 15.
The final values of the equilibrium coordinates are consistent with those determined from the empirically refined PESs, see Ref. 14: r_e = 1.0766 ± 0.0014 Ang., α_e = 134.037^o ± 0.045^o, and r_{linear} = 1.065 Ang.

The *ab initio* energies of our grid were fitted with a RMS deviation of 0.226 cm^{-1} using 66 expansion coefficients in Eq. (2). To this end, potential terms up to the 8th order were considered.

The values of the internal coordinates for each stationary point (global minimum and saddle point at the linear configuration) were found numerically through the first derivatives. As it can be seen from **Tables 1** and **2**, and according to the height of the barrier to linearity, the shape of the PES is very sensitive to both the basis set size and correction beyond the RHF-UCCSD(T) level of the theory. Such a dependence was already noticed during calculation of the height of the inversion barrier in NH_3 (see, Ref. 41 for further details).

Increasing the basis set size from ACVTZ to ACV6Z allows to gradually converge the correlation energy from the RHF-UCCSD(T) method. This becomes quite clear after a brief inspection of the height of the barrier: in the ACV6Z PES, the height is of 1933 cm^{-1}, which is about 4 cm^{-1} lower than that in the ACV5Z PES, while it is lowered by 10 cm^{-1} from ACVQZ to ACV5Z and by 34 cm^{-1} from ACVTZ to ACVQZ.

Concerning the explicitly correlated F12b method, the values of the structural parameters of the PES fall between those obtained from ACV5Z and ACV6Z. Hence, we can assume a similar behavior for the band origins. The F12a method, on the contrary, provides overestimated values of the correlation energy (see column "E_0" in **Table 1**). However, such a behavior is relevant for this method when it is combined with the CVQZ-F12 basis set (see *e.g.* the recent CH_3 work[42]). Finally, the F12a,b methods are relatively fast and quite consistent to check the convergence with respect to the size of the basis set. Indeed, computing one point requires about one hundred times less computational time than RHF-UCCSD(T)/ACV6Z.

Among all the corrections we proposed, the largest contributions in **Table 2** are sorted in this order: high-order electronic correlations, the relativistic corrections and DBOC. Finally, the height of the barrier was shifted by –8.552 cm^{-1} after adding simultaneously all these corrections. For the first time, a good agreement was reached between the *ab initio* height of the barrier (1924.6 cm^{-1}) and the empirical estimation (1931±30 cm^{-1}) obtained almost 40 years ago.[14]

3.3. Variational calculations

The nuclear motion calculations presented in this work were performed using our homemade variational computer code TENSOR based on the construction of irreducible tensor operators for the rotational, small amplitude and large amplitude vibrational parts. Following our previous works on nonrigid molecules,[41, 42] a hybrid nonrigid Hamiltonian model based on the HBJ formalism was employed. This model is described in detail in Ref. 21. The kinetic energy and potential parts were both Taylor expanded in terms of two normal mode coordinates describing the "small" vibrations (associated here with ν_1 and ν_3) for each point of a numerical grid for the nonrigid coordinate ρ describing the large amplitude motion (associated here with ν_2). The procedure[136] linking the effective coordinate ρ involved in the kinetic energy operator to the geometrically defined "real" coordinate

$\bar{\rho}$ involved in the PES was implemented in TENSOR. In order to approximately include the non-adiabatic effects, the atomic masses were employed in the kinetic energy operator (see the work by Kutzelnigg[137] for more details).

In the variational calculation, 1729 and 1547 basis functions of symmetry A_1 and B_2, respectively, was needed to achieve a convergence better than 10^{-5} cm^{-1} up to 10000 cm^{-1}. In order to check consistency of our calculation, the DVR3D computer code by Tennyson *et al.*[138] was also used. The difference between the energy levels obtained from the two computer codes is around 10^{-5} cm^{-1} up to 10000 cm^{-1} (see Ref. 21), but contrary to DVR3D, we are able to provide quite easily the vibrational and rotational quantum numbers.

4. RESULTS

4.1. Vibrational levels

Before comparing our results with experimental data, let us first analyze how our predicted band origins depend on the size of the orbital basis set. According to **Table 3**, the differences between the ACV5Z and ACV6Z PESs for the three fundamental bands of $CH_2(\tilde{X})$, namely $\nu_2(A_1)$, $\nu_1(A_1)$, and $\nu_3(B_2)$, are of –0.632 cm^{-1}, +0.452 cm^{-1}, and +0.734 cm^{-1}, respectively. We can conclude that the error for the three fundamental band centers is better than 1 cm^{-1} when using the ACV6Z PES. The reader can also see the correspondence between the height of the barrier (see **Tables 1** and **2**) and the value of the band origin for $\nu_2(A_1)$: this latter decreases as the height of the barrier decreases. As expected, the band origin of $\nu_2(A_1)$ obtained from the F12b PES lie between those provided by ACV5Z and ACV6Z calculations while it is underestimated when using the F12a PES.

TABLE 3 Impact of the orbital basis set size on the band origins of $CH_2(\tilde{X})$

Band	ACVTZ	ACVQZ	ACV5Z	ACV6Z	F12b	F12a
$\nu_2(A_1)$	968.577	965.081	963.790	963.158	963.616	960.791
$2\nu_2(A_1)$	1837.448	1831.871	1830.016	1829.128	1830.125	1825.599
$3\nu_2(A_1)$	2820.716	2820.048	2819.718	2819.336	2820.392	2817.168
$\nu_1(A_1)$	3021.146	3028.522	3031.185	3031.637	3032.565	3032.647
$\nu_3(B_2)$	3237.492	3245.849	3249.144	3249.878	3250.932	3251.319
$\nu_1+\nu_2(A_1)$	3969.381	3973.766	3975.172	3975.161	3976.461	3974.155
$4\nu_2(A_1)^*$	4017.326	4021.664	4022.821	4022.792	4024.017	4021.555
$\nu_2+\nu_3(B_2)$	4219.593	4225.209	4227.437	4227.644	4229.166	4226.911
$\nu_1+2\nu_2(A_1)$	4860.846	4862.977	4863.695	4863.294	4865.334	4860.714
$2\nu_2+\nu_3(B_2)$	5089.476	5092.337	5093.787	5093.663	5095.830	5091.347

Notes:
All *ab initio* PESs included the corrections beyond the RHF-UCCSD(T) level of the theory that were demonstrated in **Table 2.**
*for this band the contributions of the (0 4 0) and (1 1 0) basis wavefunctions were of 30 % and 34 %, respectively.

The F12a,b methods yield the results near the basis set limit accuracy already with the CVQZ-F12 basis set. Concerning the stretching $\nu_1(A_1)$ and $\nu_3(B_2)$ bands, the difference between ACV6Z and

F12a,b is below 1.5 cm^{-1}, which is rather good for such methods requiring low computational effort. Note that these methods involve approximations and do not yield the exact CCSD-F12 energies. Some improvement of the results can be obtained by scaling the triples energy contribution (see Section 22.10 in Ref. 23), which was not considered in this work where the default options were applied.

According to **Table 4**, the variational calculation using the ACV6Z PES allowed to predict accurately the band origin for the ν_2 band of the three triplet isotopologues CH_2, CD_2, and $^{13}CH_2$ with the following deviations (in cm^{-1}) to observation: –0.0585, 0.0738, and –0.0636, respectively. Our results are thus 20 times more accurate than best available ones by Császár *et al.*[20] Finally, among all the PESs we have tested in this work, the ACV6Z PES gives the most accurate results (see **Table 3)**. Concerning the asymmetric CHD molecule, for which no observed data are available, the accuracy of our predictions is presumably the same as for the other species.

TABLE 4 Fundamental band origins of four isotopologues ("Iso") of triplet methylene computed from the different *ab initio* PESs

Iso	Band	I	II	III	IV	V	This work	Exp.
CH_2	$\nu_1(A_1)$	2985.0	3013.0	3035.6	3067.5	3036.0	3031.637	–
	$\nu_2(A_1)$	967.0	969.0	964.6	942.8	967.0	963.158	963.0995(2)[a]
	$\nu_3(B_2)$	3205.0	3235.0	3248.9	3200.2	3252.0	3249.878	–
CHD	$\nu_1(A')$	–	3134.0	–	–	–	3146.318	–
	$\nu_2(A')$	–	876.0	–	–	–	867.282	–
	$\nu_3(A')$	–	2297.0	–	–	–	2308.324	–
CD_2	$\nu_1(A_1)$	2157.0	2177.0	–	–	–	2190.588	–
	$\nu_2(A_1)$	754.0	755.0	–	–	–	752.301	752.3748(16)[b]
	$\nu_3(B_2)$	2428.0	2449.0	–	–	–	2460.944	–
$^{13}CH_2$	$\nu_1(A_1)$	–	3010.0	–	–	–	3029.183	–
	$\nu_2(A_1)$	–	965.0	–	–	–	959.231	959.1674(2)[c]
	$\nu_3(B_2)$	–	3220.0	–	–	–	3234.765	–

Notes:
I – McLean *et al.*;[112] II – Comeau *et al.*;[113] III – Császár *et al.*;[20] IV – Medvedev *et al.*;[116] V – Furtenbacher *et al.*[10]
Sources of experimental data: *a* – Marshall *et al.*;[67] *b* and *c* – McKellar *et al.*[66, 71]
This work result is based on the RHF-UCCSD(T)/ACV6Z PES

The low accuracy of the previous works could be explained by as follows.

First, from *the quality of the ab initio calculations* during the construction of the PES. In the previous works by McLean *et al*. and Comeau *et al.* (columns I and II in **Table 4**), the SOCI(Q) and MRCI(Q) approaches were combined with relatively small orbital basis sets comparable to the current VTZ, VQZ or V5Z basis sets with no both augmenting polarization and core correlation functions. Accordingly, their values for the two stretching modes were underestimated because the correlation energy was poorly described. Similarly, their value for the bending mode was overestimated because of a negative contribution of the correlation energy to the height of the barrier (see **Tables 1** and **2**).

Second, from *the completeness* of the PES. Although the *ab initio* calculations by Császár *et al.*[20] and Furtenbacher *et al.*[10] (see columns III and V in **Table 4**) were done using the restricted open-

shell CC method [R(O)CCSD(T)] and the ACVQZ basis set, the anharmonic contribution was included only from the quartic force field representation of the PES. Obviously, this is not enough for quasilinear nonrigid molecules like $CH_2(\tilde{X})$. Let us note that performing calculations at the CCSD(T)/ACVQZ level of the theory remains a good choice for many molecules when corrections are not considered. In that case, the accuracy is between 5 and 10 cm^{-1} for the fundamental bands. However, to get an agreement within 1 cm^{-1} it is necessary to converge calculations with respect to the basis set and to include corrections.

The calculations of Medvedev *et al.*[116] (column IV in **Table 4**) stand apart because they were carried out for $CH_2(\tilde{X})$ in the dissociation channel of CH_3: $CH_2(\tilde{X})$+H. The band origin obtained from icMRCI(Q)/AVTZ was predicted at 942 cm^{-1} for the bending mode and is in contradiction with the height of the barrier to linearity of 2039 cm^{-1} given in Table 3 of Ref. 116. One explanation could be the quality of the fit.

Another explanation concerning the difference between the results of Császár *et al.*[20] and Furtenbacher *et al.*[10] could be the use of different nuclear-motion computer codes because their *ab initio* calculations were made using the same level of the theory. In the first paper in 2003, the so-called nonrigid-rotation large-amplitude-internal-motion Hamiltonian (NRLH) of Szalay *et al.*[139–141] was used, while the DVR3D code was used in the second paper in 2006. A different construction of the kinetic energy operator (NRLH *versus* DVR3D) may thus deviate the energy levels by several wavenumbers. In that case, it is difficult to estimate the actual accuracy of the *ab initio* PES.

TABLE 5 Vibrational energy levels (in cm^{-1}) for the four isotopologues of triplet methylene computed variationally from the *ab initio* RHF-UCCSD(T)/ACV6Z PES

CH_2	CHD	CD_2	$^{13}CH_2$
963.158 (0 1 0)	867.282 (0 1 0)	752.301 (0 1 0)	959.231 (0 1 0)
1829.128 (0 2 0)	1628.341 (0 2 0)	1414.854 (0 2 0)	1820.333 (0 2 0)
2819.336 (0 3 0)	2308.324 (0 0 1)	2048.251 (0 3 0)	2803.044 (0 3 0)
3031.637 (1 0 0)	2441.980 (0 3 0)	2190.588 (1 0 0)	3029.183 (1 0 0)
3249.878 (0 0 1)	3146.318 (1 0 0)	2460.944 (0 0 1)	3234.765 (0 0 1)
3975.161 (1 1 0)	3191.922 (0 1 1)	2792.553 (0 4 0)	3958.688 (0 4 0)
4022.792 (0 4 0)*	3416.499 (0 4 0)	2945.893 (1 1 0)	4008.766 (1 1 0)
4227.644 (0 1 1)	3941.422 (0 2 1)	3221.260 (0 1 1)	4208.197 (0 1 1)
4863.294 (1 2 0)	4040.141 (1 1 0)	3598.240 (1 2 0)	4852.394 (1 2 0)
5093.663 (0 2 1)	4505.821 (0 5 0)	3663.395 (0 5 0)	5069.745 (0 2 1)
5306.542 (0 5 0)	4557.371 (0 0 2)	3898.977 (0 2 1)	5274.580 (0 5 0)
5838.471 (1 3 0)	4741.115 (0 3 1)	4238.582 (1 3 0)	5819.444 (1 3 0)
5997.505 (2 0 0)	4817.642 (1 2 0)	4349.813 (2 0 0)	5992.152 (2 0 0)
6039.756 (0 3 1)	5414.847 (0 1 2)	4522.088 (0 3 1)	6009.535 (0 3 1)
6168.038 (1 0 1)	5472.738 (1 0 1)	4588.939 (0 6 0)	6150.681 (1 0 1)
6434.046 (0 0 2)	5577.665 (1 3 0)	4593.235 (1 0 1)	6405.276 (0 0 2)
6696.045 (0 6 0)	5644.320 (0 6 0)	4879.700 (0 0 2)	6657.723 (0 6 0)
6950.998 (2 1 0)	5771.169 (0 6 0)	4980.427 (1 4 0)	6937.435 (2 1 0)
7033.175 (1 4 0)	6188.779 (2 0 0)	5109.304 (2 1 0)	7008.601 (1 4 0)
7132.469 (1 1 1)	6204.277 (0 2 2)	5233.579 (0 4 1)	7106.279 (1 1 1)

7189.571 (0 4 1)	6346.426 (1 1 1)	5356.258 (1 1 1)	7156.830 (0 4 1)
7423.094 (0 1 2)	6520.229 (1 4 0)	5575.236 (0 7 0)	7389.680 (0 1 2)
7832.176 (2 2 0)	6743.853 (0 0 3)	5645.782 (0 1 2)	7818.846 (2 2 0)
8014.679 (1 2 1)	6752.570 (0 5 1)	5758.838 (2 2 0)	7989.050 (1 2 1)
8126.487 (0 7 0)	6966.698 (0 7 0)	5862.870 (1 5 0)	8085.000 (0 7 0)
8295.211 (0 2 2)	7005.925 (0 3 2)	6018.614 (1 2 1)	8257.369 (0 2 2)
8351.228 (1 5 0)	7065.676 (2 1 0)	6079.688 (0 5 1)	8309.765 (1 5 0)
8439.110 (0 5 1)	7143.316 (1 2 1)	6337.194 (0 2 2)	8394.664 (0 5 1)
8790.667 (2 3 0)	7578.653 (1 5 0)	6397.123 (2 3 0)	8769.080 (2 3 0)
8893.598 (3 0 0)	7613.463 (0 1 3)	6477.820 (3 0 0)	8883.925 (3 0 0)
8943.319 (1 3 1)	7704.967 (1 0 2)	6596.252 (0 8 0)	8911.894 (1 3 1)
9013.339 (3 0 1)	7819.808 (2 2 0)	6649.657 (1 3 1)	8992.172 (3 0 1)
9201.718 (0 3 2)	7858.110 (0 6 1)	6693.657 (2 0 1)	9159.372 (0 3 2)
9261.157 (1 0 2)	7911.864 (1 3 1)	6803.520 (1 6 0)	9230.898 (1 0 2)
9549.291 (1 6 0)	8035.611 (0 4 1)	6946.683 (1 0 2)	9506.370 (1 6 0)
9549.423 (0 0 3)	8282.274 (0 8 0)	6969.295 (0 3 2)	9507.941 (0 0 3)
9784.662 (0 6 1)	8397.529 (0 2 2)	6974.499 (0 6 1)	9734.861 (0 6 1)
9803.446 (0 8 0)	8468.812 (2 0 1)	7135.630 (2 4 0)	9756.717 (0 8 0)
9860.452 (4 1 0)	8594.750 (1 1 2)	7243.191 (3 1 0)	9842.370 (4 1 0)
9979.943 (3 1 1)	8610.132 (2 3 0)	7256.595 (0 0 3)	9954.239 (3 1 1)
9991.433 (1 4 0)	8700.453 (1 6 0)	7360.137 (1 4 1)	9956.232 (1 4 0)

Notes:
Vibrational assignment is given in brackets for each isotopologue as (υ_1 υ_2 υ_3). The total lists of the theoretical rovibrational energy levels can be found in **Supplementary Materials**.
ZPE (in cm^{-1}): 3731.613 (CH_2), 3250.525 (CHD), 2758.755 (CD_2), and 3720.242 ($^{13}CH_2$).
*for this band the contributions of the (0 4 0) and (1 1 0) basis wavefunctions were of 30 % and 34 %, respectively.

Finally, our full-dimensional *ab initio* RHF-UCCSD(T)/ACV6Z PES was used to predict the band origins for the four isotopologues of triplet methylene below 10000 cm^{-1} (see **Table** 5). As expected, the vibrational levels are quite close for CH_2 and $^{13}CH_2$. It is worth mentioning that the gap between the overtones of the bending mode gradually increases. This is quite unusual for "standard" triatomic molecules where the barrier to linearity is generally one order of the magnitude larger than the frequency of the bending mode. For example, for H_2O the gap between the (010) and (020) levels is of 390 cm^{-1} and is bigger than the gap between (070) and (080) because of the anharmonicity. In CH_2, on the contrary, the gap between (070) and (080) is about two times bigger than that between the first two vibrational levels.

4.2. The polyad structure and rovibrational resonances

For most of the polyatomic molecules, the energy levels are organized as small groups of strong interacting vibrational levels, called polyads. In that case, the idea of introducing so-called polyad effective Hamiltonians for the analysis of absorption spectra is well established. The effective approach still plays a key role in the assignment of high-resolution spectra of many molecules (see *e.g.* the HITRAN[142] and GEISA[143] databases). Recently, a novel methodology for obtaining the parameters of both the effective Hamiltonians and dipole moment operators has been proposed in Ref. 144 for semirigid molecules, but not yet for nonrigid molecules.

Each polyad formed by groups of nearly degenerate vibrational states is characterized by the same number P defined by multiple ratios between the normal mode frequencies. According to **Table 5**, a quite clear polyad scheme occurs for CH_2: $\nu_1 \approx 3\nu_2 \approx \nu_3$. As a result, the vibrational levels inside a given polyad can be labeled by the additional polyad number, $P = 3\upsilon_1 + \upsilon_2 + 3\upsilon_3$. Such a polyad structure is quite unusual for semirigid nonlinear triatomic molecules like H_2O, H_2S, SO_2, NO_2, etc. for which we have $P=2\upsilon_1 + \upsilon_2 + 2\upsilon_3$.

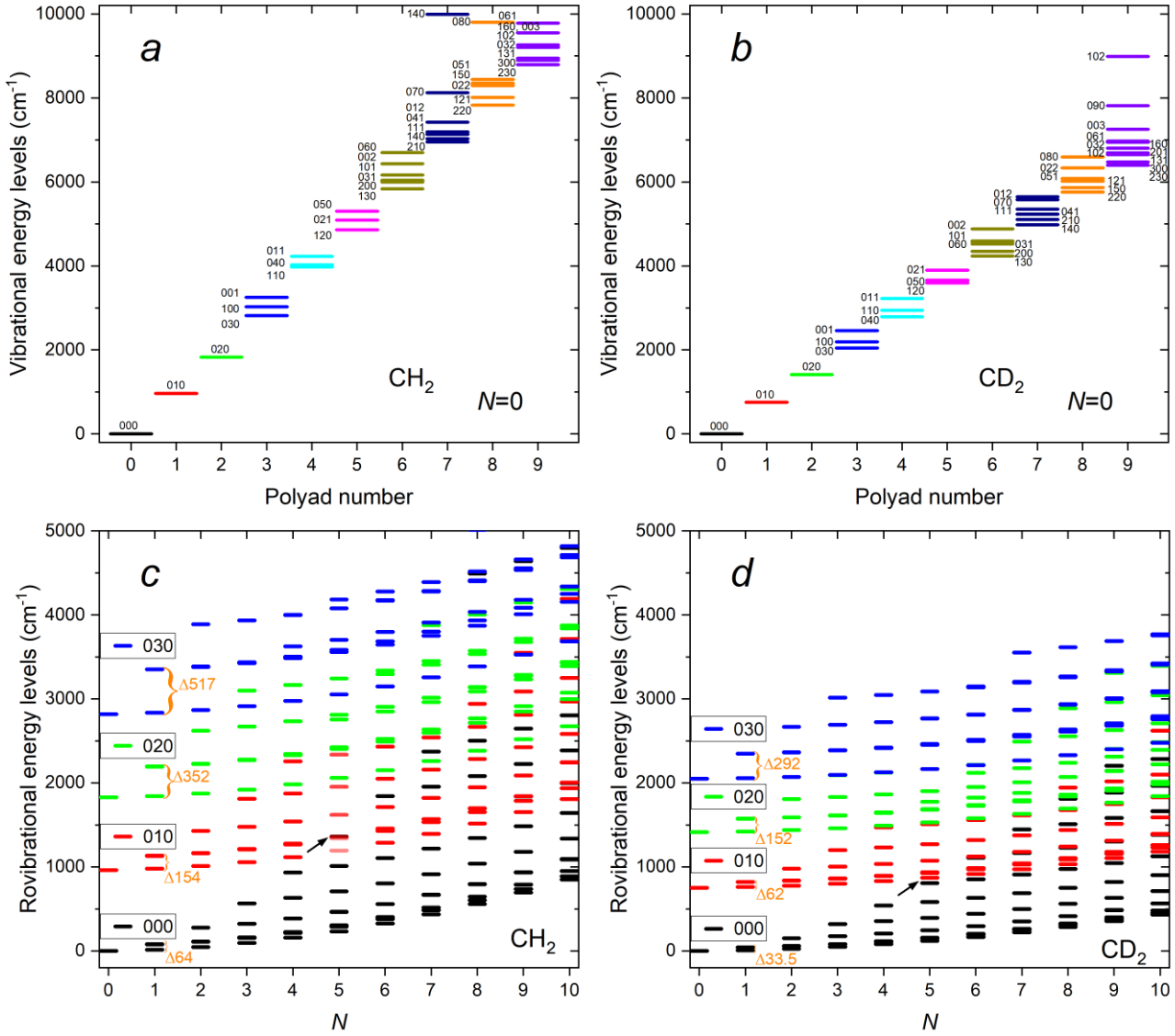

FIGURE 2 (Panels *a* and *b*) Polyad structure for the vibrational levels ($N = 0$) of $CH_2(\tilde{X})$ and $CD_2(\tilde{X})$ assuming the polyad number, $P = 3\upsilon_1 + \upsilon_2 + 3\upsilon_3$. (Panels *c* and *d*) Rovibrational energies as a function of N. The curly brackets are used to show the energy differences between the levels with $K_a = 0$ and $N = K_a$ at $N = 1$. We can see the various overlapping between the energy levels of the (000) and (010) states after $N = 5$

As displayed in **Figures 2*a*** and **2*b***, the first three polyads of $CH_2(\tilde{X})$ and $CD_2(\tilde{X})$ consist of single vibrational states and the next three polyads consist of three vibrational states (also called triads). The seventh polyad (P=6) corresponds to an hexad (six vibrational states) for both

isotopologues, while the polyad structure is becoming unclear above for $CH_2(\tilde{X})$, because of various overlapping. For $CD_2(\tilde{X})$ the inter-polyad couplings occur from the ninth polyad (P = 8).

Thus, it is possible to define quite easily a polyad scheme for $CH_2(\tilde{X})$ up to P = 5 and build the corresponding effective vibrational Hamiltonian. However, due to the large values of the rotational constants, the difficulty grows very rapidly as N increases. The rotational constant A also increases with the vibrational excitation of the bending mode. Its value is proportional to the energy difference between the levels with K_a = 0 and K_a = 1 at N = 1. Concerning the heaviest molecule, $CD_2(\tilde{X})$, the value of the rotational constant A is about two times less than that of $CH_2(\tilde{X})$, which is confirmed by the observations (see *e.g.* Tables II and III in Refs. 66 and 67).

As shown in **Figures 2*c*** and **2*d*,** a clear polyad structure is rapidly lost from $N > 4$, making problematic the construction of effective Hamiltonians. It is worth stressing the fact that such an overlapping between rovibrational states exists for most of the molecules, but occurs generally for higher excited polyads.

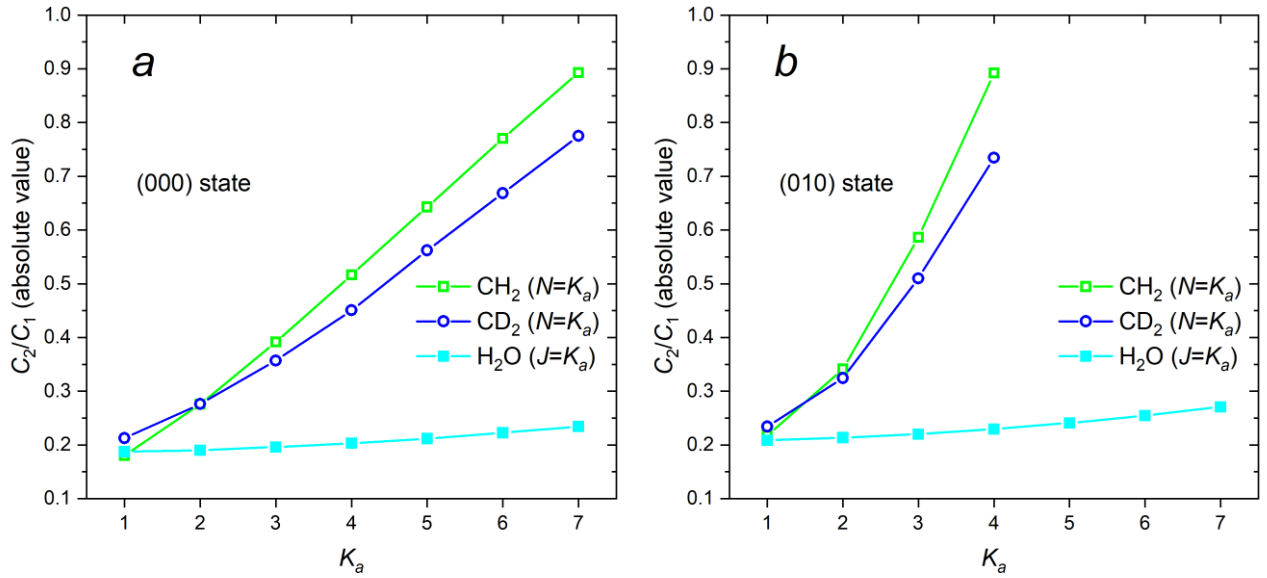

FIGURE 3 Plot of the ratio of the first (C_1) and second (C_2) biggest expansion coefficients of the rovibrational wavefunction of the (000) (*a*) and (010) (*b*) states of triplet CH_2 and CD_2 in comparison with H_2O

In order to show the strong coupling between rotation-bending states, we have plotted in **Figure 3** the ratio of the two largest mixing coefficients in the eigenfunction decomposition obtained from the variational calculation as the function of K_a. When the ratio is close to 1, the coupling between the rotation-bending states is strong and makes assignments ambiguous. As we can see, the mixing grows rapidly as a function of K_a for the (000) state of $CH_2(\tilde{X})$. For example, at N=K_a=5 the magnitudes of the two largest coefficients are of –0.792 and –0.509 while at N=K_a=7 they are much closer, –0.661 and –0.590, respectively. This behavior for the (010) state is more pronounced. As an illustration, we have also plotted in **Figure 3** these ratios for the H_2O molecule. Up to K_a=7, needless

to say that H_2O exhibits a smooth behavior compared to CH_2 and CD_2 and could be considered as a "normal" semirigid molecule. Note that some energy levels with $N=K_a > 4$ are missing in **Figure 3*b*** because of an unclear assignment in our variational calculation (see **Supplementary materials** for more details about the assignments**)**.

4.3. Rovibrational transitions

In **Table 6,** we compare the calculated rovibrational transitions with available empirical data. Our *ab initio* PES allows to reach a RMS deviation of 0.112 cm^{-1}, which is almost twenty times better than the previous *ab initio* results by Furtenbacher *et al.*[10] Our RMS error is comparable with the RMS deviation of 0.11 cm^{-1} obtained by Jensen *et al.*[15] from an empirically refined PES. Moreover, our calculations cover a wider range of vibrational and rotational quantum numbers and include the main isotopologues.

TABLE 6 A*b initio* rovibrational transitions of triplet methylene calculated in this work and by Furtenbacher *et al.*[10] in comparison with the available empirical data (Emp.)

CH_2: (000)←(000)				**CH_2: (010)←(000)**			
$N''_{K_a''K_c''} \leftarrow N'_{K_a'K_c'}$	Emp.	Emp.–Calc.		$N''_{K_a''K_c''} \leftarrow N'_{K_a'K_c'}$	Emp.	Emp.–Calc.	
		Ref. 10	This work			Ref. 10	This work
4_{04}←3_{13}	2.3104	-0.566	-0.085	8_{08}←7_{17}	1032.4728	–	-0.131
2_{12}←3_{03}	14.7873	0.558	0.084	4_{14}←5_{05}	1032.9928	-1.735	0.223
5_{05}←4_{14}	19.7808	-0.574	-0.085	9_{09}←8_{18}	1050.1838	–	-0.129
1_{11}←2_{02}	31.4467	0.553	0.083	10_{010}←9_{19}	1068.0581	–	-0.122
1_{10}←1_{01}	63.8826	0.549	0.083	2_{12}←3_{03}	1068.2735	-1.733	0.218
2_{11}←2_{02}	65.1649	0.545	0.082	1_{11}←2_{02}	1085.1470	-1.731	0.218
3_{12}←3_{03}	67.1149	0.538	0.080	2_{11}←2_{02}	1118.8696	-1.750	0.213
4_{13}←4_{04}	69.7632	0.529	0.079	3_{12}←3_{03}	1120.7315	-1.766	0.215
6_{15}←6_{06}	77.3110	0.501	0.073	5_{14}←5_{05}	1126.5534	-1.824	0.215
1_{11}←0_{00}	78.3211	0.553	0.083	6_{15}←6_{06}	1130.6264	–	0.217
2_{12}←1_{01}	92.8254	0.558	0.083	1_{11}←0_{00}	1132.0200	-1.855	0.216
4_{22}←5_{15}	97.5430	0.975	0.163	7_{16}←7_{07}	1135.5658	–	0.215
3_{22}←4_{13}	97.7342	1.037	0.174	8_{17}←8_{08}	1141.4324	–	0.213
5_{23}←5_{14}	158.5792	1.045	0.173	2_{12}←1_{01}	1146.3117	-1.730	0.218
5_{42}←4_{31}	382.4364	1.094	0.236	3_{13}←2_{02}	1159.9406	-1.732	0.220
6_{43}←5_{32}	398.5730	1.101	0.241	4_{14}←3_{03}	1172.9343	-1.731	0.222
6_{42}←5_{33}	398.5674	1.089	0.229	**CD_2: (000)←(000)**			
7_{44}←6_{33}	414.7015	1.098	0.236	1_{11}←2_{02}	17.1920	0.230	0.014
7_{43}←6_{34}	414.7175	1.096	0.235	1_{10}←1_{01}	33.5554	0.238	0.017
CH_2: (100)←(100)				2_{11}←2_{02}	34.1038	0.238	0.018
1_{10}←1_{01}	59.9423	–	0.076	3_{12}←3_{03}	34.9365	0.236	0.018
2_{11}←2_{02}	61.2095	–	0.075	1_{11}←0_{00}	40.9556	0.246	0.019
3_{12}←3_{03}	63.1389	–	0.073	2_{12}←1_{01}	48.3728	0.252	0.021
2_{12}←1_{01}	88.4156	–	0.076	3_{13}←2_{02}	55.5373	0.260	0.023
CH_2: (010)←(000)				4_{22}←5_{15}	58.9443	0.527	0.036
4_{14}←5_{23}	801.2638	-3.301	-0.029	3_{22}←4_{13}	60.1329	0.553	0.037
6_{06}←7_{17}	802.5901	–	-0.143	2_{21}←3_{12}	69.0165	0.554	0.039
4_{13}←5_{24}	814.4573	-3.366	-0.032	5_{15}←4_{04}	69.1425	0.278	0.027
5_{05}←6_{16}	815.3156	–	-0.145	5_{23}←5_{14}	90.9683	0.575	0.044

$5_{24}\leftarrow6_{33}$	815.4803	-2.174	0.023	$4_{22}\leftarrow4_{13}$	92.0210	0.572	0.045
$3_{13}\leftarrow4_{22}$	820.2705	-3.303	-0.032	$3_{21}\leftarrow3_{12}$	92.9054	0.569	0.045
$3_{12}\leftarrow4_{23}$	828.1105	-3.337	-0.033	$2_{20}\leftarrow2_{11}$	93.5938	0.567	0.045
$4_{04}\leftarrow5_{15}$	828.4198	-4.410	-0.146	$3_{22}\leftarrow3_{13}$	96.0123	0.560	0.046
$4_{22}\leftarrow5_{33}$	831.7019	-2.167	0.017	$4_{23}\leftarrow4_{14}$	97.1510	0.558	0.046
$4_{23}\leftarrow5_{32}$	831.6805	-2.162	0.017	$3_{22}\leftarrow2_{11}$	117.4458	0.583	0.051
$3_{03}\leftarrow4_{14}$	841.9163	–	-0.143	**CD_2: (010)←(010)**			
$2_{11}\leftarrow3_{22}$	842.2978	-3.318	-0.037	$1_{11}\leftarrow2_{02}$	45.8637	0.347	0.041
$3_{22}\leftarrow4_{31}$	847.8123	-2.150	0.016	$2_{11}\leftarrow2_{02}$	62.7231	0.887	0.046
$3_{21}\leftarrow4_{32}$	847.8195	-2.152	0.016	$3_{12}\leftarrow3_{03}$	63.6418	0.898	0.046
$10_{010}\leftarrow10_{19}$	855.5925	–	-0.092	$1_{11}\leftarrow0_{00}$	69.4368	0.903	0.048
$1_{11}\leftarrow2_{20}$	855.7320	-3.298	-0.035	$2_{12}\leftarrow1_{01}$	76.8260	0.901	0.049
$2_{02}\leftarrow3_{13}$	855.8054	-4.365	-0.143	$3_{13}\leftarrow2_{02}$	83.9800	0.907	0.051
$1_{10}\leftarrow2_{21}$	857.0167	-3.304	-0.036	$4_{14}\leftarrow3_{03}$	90.9033	0.929	0.053
$9_{09}\leftarrow9_{18}$	863.5033	–	-0.104	$2_{21}\leftarrow3_{12}$	117.0708	1.372	0.058
$2_{20}\leftarrow3_{31}$	863.8719	-2.140	0.016	$3_{21}\leftarrow3_{12}$	140.8969	1.385	0.065
$7_{17}\leftarrow7_{26}$	866.8280	–	-0.016	$2_{20}\leftarrow2_{11}$	141.5486	1.483	0.064
$1_{01}\leftarrow2_{12}$	870.0952	-4.348	-0.141	$2_{21}\leftarrow2_{12}$	143.1560	1.371	0.065
$8_{08}\leftarrow8_{17}$	870.6924	–	-0.111	$2_{21}\leftarrow1_{10}$	157.8676	1.383	0.068
$6_{16}\leftarrow6_{25}$	872.0183	–	-0.021	$2_{20}\leftarrow1_{11}$	158.4080	1.384	0.069
$5_{15}\leftarrow5_{24}$	876.5200	–	-0.026	**CD_2: (100)←(100)**			
$7_{07}\leftarrow7_{16}$	877.1265	–	-0.116	$3_{22}\leftarrow2_{11}$	117.1872	–	0.048
$4_{14}\leftarrow4_{23}$	880.3110	-3.303	-0.028	**CD_2: (010)←(000)**			
$6_{06}\leftarrow6_{15}$	882.7805	–	-0.124	$3_{03}\leftarrow3_{12}$	717.0699	–	0.062
$3_{13}\leftarrow3_{22}$	883.3664	-3.303	-0.032	$4_{04}\leftarrow4_{13}$	715.7102	–	0.064
$0_{00}\leftarrow1_{11}$	884.7780	–	-0.143	$5_{05}\leftarrow5_{14}$	713.9986	–	0.064
$2_{12}\leftarrow2_{21}$	885.6730	-3.299	-0.035	$6_{06}\leftarrow6_{15}$	711.9297	–	0.063
$5_{05}\leftarrow5_{14}$	887.6467	–	-0.128	$7_{07}\leftarrow7_{16}$	709.4992	–	0.063
$2_{11}\leftarrow2_{20}$	889.4580	-3.314	-0.036	**$^{13}CH_2$: (010)←(000)**			
$3_{12}\leftarrow3_{21}$	890.8735	-3.333	-0.036	$3_{13}\leftarrow3_{22}$	879.8830	–	-0.050
$4_{04}\leftarrow4_{13}$	891.7090	-4.344	-0.133	$0_{00}\leftarrow1_{11}$	881.7530	–	-0.166
$4_{13}\leftarrow4_{22}$	892.6835	–	-0.035	$2_{11}\leftarrow2_{20}$	886.0130	–	-0.053
$5_{14}\leftarrow5_{23}$	894.8265	-3.388	-0.034	$3_{12}\leftarrow3_{21}$	887.4390	–	-0.054
$2_{02}\leftarrow2_{11}$	897.4080	-4.340	-0.139	$4_{04}\leftarrow4_{13}$	888.6370	–	-0.156
$1_{01}\leftarrow1_{10}$	899.0370	–	-0.142	$3_{03}\leftarrow3_{12}$	891.9050	–	-0.160
$5_{24}\leftarrow5_{33}$	910.1390	-2.168	0.021	$2_{02}\leftarrow2_{11}$	894.3580	–	-0.163
$5_{23}\leftarrow5_{32}$	910.1660	-2.178	0.020	$1_{01}\leftarrow1_{10}$	895.9940	–	-0.165
$4_{23}\leftarrow4_{32}$	910.6279	-2.153	0.020	$2_{02}\leftarrow1_{11}$	928.0780	–	-0.165
$4_{22}\leftarrow4_{31}$	910.6406	-2.159	0.018	$3_{03}\leftarrow2_{12}$	944.2500	–	-0.164
$3_{22}\leftarrow3_{31}$	911.0095	-2.144	0.016	**CHD: (000)←(000)**			
$3_{13}\leftarrow2_{20}$	930.5250	-3.300	-0.033	$3_{13}\leftarrow4_{04}$	4.4189[a]	–	0.030
$2_{02}\leftarrow1_{11}$	931.1260	-4.348	-0.141	$5_{05}\leftarrow4_{14}$	7.3681[a]	–	-0.041
$3_{03}\leftarrow2_{12}$	947.2910	-4.376	-0.141	$2_{12}\leftarrow3_{03}$	15.9644[a]	–	0.028
$8_{17}\leftarrow7_{26}$	1030.7219	–	-0.030	$6_{06}\leftarrow5_{15}$	19.3912[b]	–	-0.031
				$7_{07}\leftarrow6_{16}$	31.5825[b]	–	-0.030
RMS						**2.091**	**0.112**

Notes:
All empirical data except for CHD were taken from Table I of Jensen *et al.*[15] These rovibrational transitions were obtained by removing the fine and hyperfine structures (see *e.g.* Refs. 14 and 15 for further details).
The empirical rovibrational transitions for CHD were obtained in this work using the empirical parameters from the following papers: *a* – Ref. 119 and *b* – Ref. 120 (see details in the text).
The total lists of the theoretical rovibrational energy levels are given in **Supplementary Materials**.

1

Note that the differences between the "observed" and calculated transitions in **Table 6** are not regular. Concerning the heaviest $CD_2(\tilde{X})$ molecule, the agreement is undoubtedly better. For example, deviations of 0.174 and 0.037 cm^{-1} may occur for the same pure rotational $3_{22}\leftarrow4_{13}$ transition of $CH_2(\tilde{X})$ and $CD_2(\tilde{X})$, respectively, and cannot be explained by some resonances. According to **Figure 3**, the mixing coefficients are close for both isotopologues. Even for the (010)-(000) transitions of $CH_2(\tilde{X})$, the deviations are far to be regular, going from –0.016 to –0.141 cm^{-1} for $7_{17}\leftarrow7_{26}$ and $1_{01}\leftarrow2_{12}$, respectively. These two transitions were measured by Marshall & McKellar[67] and we can note from their Table I that the splitting due to the fine structure was several times bigger for $1_{01}\leftarrow2_{12}$ than for $7_{17}\leftarrow7_{26}$. For example, the separation between the F_2 (S=0) and F_3 (S=–1) components were of –0.1054 and +0.5021 cm^{-1} for $7_{17}\leftarrow7_{26}$ and $1_{01}\leftarrow2_1$, while the F_1 (S=+1) component was shifted from F_2 by –0.0919 and +0.1233 cm^{-1}, respectively.

Consequently, the irregularities between the "observed" and calculated transitions can be partly explained by the difference in the magnitude of the electron spin splitting, which was removed in the empirical rovibrational transitions presented in **Table 6.** Indeed, the empirical transitions were obtained by setting to zero the spin-spin and spin-rotation parameters in the effective Hamiltonian. This corroborates the fact that the spin-rotation parameters (ε_{aa}, ε_{bb}, and ε_{cc}) of $CD_2(\tilde{X})$ are about two times smaller than those of $CH_2(\tilde{X})$ (see *e.g.* Table 2 in Ref. 114).

For this work, we have also calculated the empirical rovibrational transitions for the $CHD(\tilde{X})$ isotopologue. To this end, the SPCAT program of Pickett[145] was employed and the empirical parameters of the effective Hamiltonian determined by Nolte *et al.*[119] and Ozeki *et al.*[120] were used. The fine and hyperfine contributions were not included here. The obtained empirical line positions of the five rovibrational transitions are in very good agreement with our calculations (see the end of **Table 6**).

Before making predictions for $CHD(\tilde{X})$, we first made trial tests using the empirical parameters of $CH_2(\tilde{X})$ given in Table III of Ref. 63 in order to obtain the same results as those presented in the column "Observed" of Table IV of Ref. 63. Moreover, this corroborated the fact that the spin-spin and spin-rotation parameters were not considered to build the "Emp." column of **Table 6.**

4.4. Comparison with the generating-function approach

Although the effective Watson Hamiltonian was used to fit the observed line positions of triplet methylene (see Section 2), the anomalously large centrifugal distortion of CH_2 makes the predictions rapidly unreliable. Indeed, the conventional power series expansion of the Hamiltonian rapidly fails. For that reason, Bunker, Jensen *et al*. preferred using the variational approach to compute rovibrational levels.

Alternative methods were proposed to improve the convergence of the effective Hamiltonian, based for example on the Padé and Borel approximants (see *e.g.* Burenin *et al.*,[146] Polyansky *et al.*,[147] and Belov *et al.*[148]). In the SPFIT and SPCAT programs of Pickett, the Euler series was implemented for this purpose (more details are given in Ref. 149). Another approach based on the use of generating functions was proposed by Tyuterev and Starikov.[150, 151] In Ref. 152, the generating functions combined with the Borel-type summation were used to predict $CH_2(\tilde{X})$ energy levels. As an illustrative example, we have compared the ground vibrational state energy levels of $CH_2(\tilde{X})$ obtained from variational calculations (This work), from the generating function approach and from the Watson Hamiltonian (see **Table 7**).

TABLE 7 Rotational energy levels of the ground vibrational state of $CH_2(\tilde{X})$ calculated in this work and compared to those predicted by Starikov and Mikhailenko[152] using different effective approaches

$N_{K_aK_c}$	This work		This work – Ref. 152	
	Energy	C_2/C_1	"standard" Watson	generating function
1_{01}	15.63	0.157	0.00	0.00
1_{11}	78.24	0.180	-0.10	-0.10
1_{10}	79.43	0.180	1.09	-0.09
2_{02}	46.87	0.158	0.01	-0.01
2_{12}	108.38	0.180	-0.08	-0.10
2_{11}	111.96	0.178	-0.06	-0.07
2_{21}	276.02	0.276	-0.11	-0.26
2_{20}	276.04	0.276	-0.11	-0.25
3_{03}	93.67	0.159	0.03	-0.01
3_{13}	153.56	0.179	-0.04	-0.10
3_{12}	160.71	0.176	-0.02	-0.06
3_{22}	323.20	0.273	-0.10	-0.23
3_{21}	323.28	0.274	-0.11	-0.24
3_{31}	566.64	0.391	18.96	1.40
3_{30}	566.64	0.391	18.95	1.40
4_{04}	155.95	0.161	0.05	-0.01
4_{14}	213.75	0.178	0.01	-0.09
4_{13}	225.64	0.173	0.01	-0.05
4_{23}	386.05	0.272	-0.09	-0.19
4_{22}	386.29	0.272	-0.12	-0.23
4_{32}	629.83	0.390	18.87	1.45
4_{31}	629.84	0.390	18.88	1.46
4_{41}	932.73	0.516	18.67	1.13
4_{40}	932.73	0.516	18.67	1.13
5_{05}	233.61	0.164	0.06	-0.01
5_{15}	288.91	0.176	0.08	-0.07
5_{14}	306.69	0.168	0.04	-0.06
5_{24}	464.52	0.269	-0.09	-0.16
5_{23}	465.09	0.269	-0.16	-0.23
5_{33}	708.77	0.388	18.75	1.51
5_{32}	708.78	0.388	18.75	1.51
5_{42}	1012.04	0.514	18.63	1.21

5_{41}	1012.04	0.514	18.63	1.21
5_{51}	1361.62	0.643	-239.08	-5.61
5_{50}	1361.62	0.643	-239.08	-5.61
6_{06}	326.54	0.167	0.09	0.00
6_{16}	379.00	0.174	0.20	-0.01
6_{15}	403.78	0.172	0.04	-0.10
6_{25}	558.57	0.266	-0.09	-0.11
6_{24}	559.70	0.267	-0.24	-0.25
6_{34}	803.42	0.384	18.56	1.56
6_{33}	803.43	0.384	18.55	1.55
6_{43}	1107.11	0.511	18.52	1.28
6_{42}	1107.11	0.511	18.52	1.28
6_{52}	1457.14	0.641	-238.47	-5.54
6_{51}	1457.14	0.640	-238.47	-5.54
6_{61}	1844.06	0.770	-1390.88	-22.83
6_{60}	1844.06	0.770	-1390.88	-22.83

Notes:
Here "standard" Watson means the effective *A*-reduced Watson Hamiltonian. For further details concerning the generating function approach see Ref. 152.
To demonstrate the mixing between the basis states we give the C_2/C_1 ratio, where C_1 and C_2 are the first and second biggest expansion coefficients of the rovibrational wavefunction of the ground vibrational state.

As expected, the "standard" Watson Hamiltonian dramatically failed to predict the pure rotational energy levels. Even at $N = K_a = 3$, the disagreement is of –19 cm^{-1} while at $N = K_a = 6$ it is of –1391 cm^{-1}. The generating function approach gives more consistent results, with a smoother behavior, though the disagreements with our calculations remains quite large: –23 cm^{-1} at $N = K_a = 6$. We did not compare our results to those obtained using the Euler series approach of Pickett. However, according to Figure 3 of Ref. 9, we can conclude that the Euler series approach does not allow to drastically improve the quality of the predictions.

In **Table 7** we can see that the mixing between eigenfunctions (estimated as C_2/C_1) strongly depends on K_a. The ratio is quite similar for different states with the same value of K_a. Similar results were obtained using the effective approaches with for example a deviation of – 5.54 cm^{-1} for the state 6_{51} and a deviation of –5.61 cm^{-1} for the state 5_{51}. As expected, there is clearly a correlation between the magnitude of the deviation and that of the mixing.

5. CONCLUSIONS

In this work, an accurate *ab initio* PES for the quasilinear triplet ($\tilde{X}^3B_1$) methylene was built using the RHF-UCCSD(T)/aug-cc-pCV6Z method and including the corrections due to the scalar relativistic effects, DBOC and high-order electronic correlations. For the first time, the *ab initio* height of the barrier to linearity (1924.6 cm^{-1}) agrees well with that obtained from the empirical PES published almost 40 years ago (1931±30 cm^{-1}). All the available experimental band origins for the three isotopologues CH_2, CD_2, and $^{13}CH_2$ were reproduced with an accuracy below 0.1 cm^{-1} while

the RMS deviation between calculated and empirical transitions, including those for CHD, was of 0.112 cm^{-1}.

Moreover, our variational calculations for rovibrational energy levels up to ~10000 cm^{-1} allowed to analyze the overall polyad structure, and the polyad number $P = 3\upsilon_1 + \upsilon_2 + 3\upsilon_3$ was proposed. However, the rovibrational resonance interactions between the polyads grow very rapidly as K_a increases because of the extremely large rotational and centrifugal distortion constants of triplet methylene. We have noted a strong mixing from $K_a = 5$, even for the ground vibrational state (000) making unusable traditional Watson-based effective Hamiltonians. We can thus conclude that the variational approach is probably better suited than the effective approach to compute the $CH_2(\tilde{X}^3B_1)$ spectra.

ACKNOWLEDGEMENTS

This work was supported by the Russian Scientific Foundation (RSF, No. 22-42-09022) and by the French ANR "TEMMEX" project (Grant 21-CE30-0053-01). The support from the ROMEO computer center of Reims-Champagne-Ardenne is also acknowledged.

This work is dedicated to Professor Per Jensen who is gratefully acknowledged for the fruitful discussions he shared with the authors during his visit in Reims.

SUPPLEMENTARY MATERIALS

We provide the complete list of the rovibrational energy levels of the four isotopologues of triplet methylene calculated variationally up to ~10000 cm^{-1}. The C++ and Fortran codes for computing potential energies from the final *ab initio* PES. The *ab initio* points of the potential energies for 1150 nuclear configurations calculated in this work.

REFERENCES

[1] M. A. Blitz, P. W. Seakins, *Chem. Soc. Rev.* **2012**, *41*, 6318. https://doi.org/10.1039/C2CS35204D

[2] B. Gans, S. Boyé-Péronne, M. Broquier, M. Delsaut, S. Douin, C. E. Fellows, P. Halvick, J.-C. Loison, R. R. Lucchese, D. Gauyacq, *Phys. Chem. Chem. Phys.* **2011**, *13*, 8140. https://doi.org/10.1039/C0CP02627A

[3] K. M. Douglas, M. A. Blitz, W. Feng, D. E. Heard, J. M.C. Plane, H. Rashid, P. W. Seakins, *Icarus* **2019**, *321*, 752. https://doi.org/10.1016/j.icarus.2018.12.027

[4] J. M. Hollis, P. R. Jewell, F. J Lovas, *The Astrophysical Journal* **1995**, *438*, 259. https://doi.org/10.1086/175070

[5] E. T. Polehampton, K. M. Menten, S. Brünken, G. Winnewisser, J.-P. Baluteau, *A&A* **2005**, *431*, 203. https://doi.org/10.1051/0004-6361:20041598

[6] F. J. Lovas, R. D. Suenram, K. M. Evenson, *Astrophys. J. Lett.* **1983**, *267*, L131. https://doi.org/10.1086/184017

[7] E. A. Michael, F. Lewen, G. Winnewisser, H. Ozeki, H. Habara, E. Herbst, *The Astrophysical Journal* **2003**, *596*, 1356. https://doi.org/10.1086/378090

[8] S. Brünken, E. A. Michael, F. Lewen, Th. Giesen, H. Ozeki, G. Winnewisser, P. Jensen, E. Herbst, *Can. J. Chem.* **2004**, *82*, 676. https://doi.org/10.1139/v04-034

[9] S. Brünken, H. S. P. Müller, F. Lewen, T. F. Giesen, *J. Chem. Phys.* **2005**, *123*, 164315. https://doi.org/10.1063/1.2074467
[10] T. Furtenbacher, G. Czakó, B. T. Sutcliffe, A. G. Császár, V. Szalay, *J. Mol. Structure.* **2006**, *780–781*, 283. https://doi.org/10.1016/j.molstruc.2005.06.052
[11] L. H. Coudert, *J. Chem. Phys.* **2020,** *153*, 144115 https://doi.org/10.1063/5.0026162
[12] P. Jensen, P. R. Bunker, A. R. Hoy, *J. Chem. Phys.* **1982**, *77*, 5370 https://doi.org/10.1063/1.443785
[13] P. R. Bunker, P. Jensen, *J. Chem. Phys.* **79,** 1224 (1983) http://dx.doi.org/10.1063/1.445927
[14] P. R. Bunker, P. Jensen, W. P. Kraemer, R. Beardsworth, *J. Chem. Phys.* **85,** 3724 (1986) https://doi.org/10.1063/1.450944
[15] P. Jensen, P. R. Bunker, *J. Chem. Phys*. **89,** 1327 (1988) https://doi.org/10.1063/1.455184
[16] P. Jensen, *J. Mol. Spectrosc.* **128**, 478 (1988) https://doi.org/10.1016/0022-2852(88)90164-6
[17] V. J. Barclay, I. P. Hamilton, P. Jensen, *J. Chem. Phys.* **99,** 9709 (1993) https://doi.org/10.1063/1.465453
[18] *Recent advances in coupled-cluster methods*, edited by R. J. Bartlett, World Scientific Publishing Company **1997**, 340. https://doi.org/10.1142/3455
[19] *Recent Progress in Coupled Cluster Methods: Theory and Applications in Challenges and Advances in Computational Chemistry and Physics*, edited by P. Cársky, J. Paldus, J. Pittner, Springer **2010**, 657. https://doi.org/10.1007/978-90-481-2885-3
[20] A. G. Császár, M. L. Leininger, V. Szalay, *J. Chem. Phys*. **2003**, *118*, 10631. https://doi.org/10.1063/1.1573180
[21] M. Rey, D. Viglaska, O. Egorov, A. V. Nikitin, *J. Chem. Phys*. 2023 (under revision).
[22] H.-J. Werner, P. J. Knowles, F. R. Manby, J. A. Black, K. Doll, A. Heßelmann, D. Kats, A. Köhn, T. Korona, D. A. Kreplin, Q. Ma, T. F. Miller, A. Mitrushchenkov, K. A. Peterson, I. Polyak, G. Rauhut, M. Sibaev, *J. Chem. Phys*. **2020**, *152*, 144107. https://doi.org/10.1063/5.0005081
[23] H.-J. Werner, P. J. Knowles, G. Knizia, F. R. Manby, M. Schütz et al. MOLPRO, version 2019.2, a package of ab initio programs, https://www.molpro.net (accessed April 6, 2023).
[24] M. Kállay, P. R. Nagy, D. Mester, Z. Rolik, G. Samu, J. Csontos, J. Csóka, P. B. Szabó, L. Gyevi-Nagy, B. Hégely, I. Ladjánszki, L. Szegedy, B. Ladóczki, K. Petrov, M. Farkas, P. D. Mezei, A. Ganyecz, *J. Chem. Phys*. **2020**, *152*, 074107. https://doi.org/10.1063/1.5142048
[25] M. Kállay, P. R. Nagy, D. Mester, Z. Rolik, G. Samu, J. Csontos, J. Csóka, P. B. Szabó, L. Gyevi-Nagy, B. Hégely, I. Ladjánszki, L. Szegedy, B. Ladóczki, K. Petrov, M. Farkas, P. D. Mezei, Á. Ganyecz, MRCC, a quantum chemical program suite, https://www.mrcc.hu (accessed April 6, 2023).
[26] D. A. Matthews, L. Cheng, M. E. Harding, F. Lipparini, S. Stopkowicz, T. -C. Jagau, P. G. Szalay, J. Gauss, J. F. Stanton, *J. Chem. Phys*. **2020**, *152*, 214108. https://doi.org/10.1063/5.0004837
[27] J. F. Stanton, J. Gauss, L. Cheng, M. E. Harding, D. A. Matthews, P. G. Szalay, A. A. Auer, R. J. Bartlett, U. Benedikt, C. Berger et al. CFOUR, a quantum chemical program package, http://www.cfour.de (accessed April 6, 2023).
[28] M. Rey, A. V. Nikitin, Vl. G. Tyuterev, *Mol. Phys.* **2010**, *108*, 2121 https://doi.org/10.1080/00268976.2010.506892
[29] M. Rey, A. V. Nikitin, Vl. G. Tyuterev, *J. Chem. Phys*. **2012**, *136*, 244106. https://doi.org/10.1063/1.4730030
[30] M. Rey, *J. Chem. Phys*. **2019**, *151*, 024101. https://doi.org/10.1063/1.5109482
[31] T. Delahaye, A. Nikitin, M. Rey, P. G. Szalay, Vl. G. Tyuterev, *J. Chem. Phys*. **2014**, *141*, 104301. https://doi.org/10.1063/1.4894419
[32] T. Delahaye, A. Nikitin, M. Rey, P. G. Szalay, Vl. G. Tyuterev, *Chem. Phys. Lett.* **2015**, *639*, 275. https://doi.org/10.1016/j.cplett.2015.09.042
[33] M. Rey, A. Nikitin, A. Campargue, S. Kassi, D. Mondelain, V. Tyuterev, *Phys. Chem. Chem. Phys.* **2016**, *18*, 176. https://doi.org/10.1039/C5CP05265C
[34] M. Rey, A. V. Nikitin, Y. L. Babikov, V. G. Tyuterev, *J. Mol. Spectrosc.* **2016**, *327*, 138. https://doi.org/10.1016/j.jms.2016.04.006
[35] M. Rey, A.V. Nikitin, V.G. Tyuterev, *The Astrophysical Journal* 2017, *847*, 105. https://doi.org/10.3847/1538-4357/aa8909
[36] M. Rey, I. S. Chizhmakova, A. V. Nikitin, V. G. Tyuterev, *Phys. Chem. Chem. Phys*. **2018**, *20*, 21008. https://doi.org/10.1039/C8CP03252A
[37] D. Viglaska, M. Rey, A.V. Nikitin, V. G. Tyuterev, *J. Chem. Phys*. **2018**, *149*, 174305. https://doi.org/10.1063/1.5045525

[38] O. Egorov, A. Nikitin, M. Rey, A. Rodina, S. Tashkun, V. Tyuterev, *J. Quant. Spectrosc. Radiat. Transfer* **2019**, *239*, 106668. https://doi.org/10.1016/j.jqsrt.2019.106668
[39] D. Viglaska-Aflalo, M. Rey, A. Nikitin, T. Delahay, *Phys. Chem. Chem. Phys.* **2020**, *22*, 3204. https://doi.org/10.1039/C9CP06383H
[40] M. Rey, I.S. Chizhmakova, A.V. Nikitin, V.G. Tyuterev, *Phys. Chem. Chem. Phys.* **2021**, *23*, 12115. https://doi.org/10.1039/D0CP05727D
[41] O. Egorov, M. Rey, A. Nikitin, V. Dominika, *J. Phys. Chem. A* **2021**, *125*, 10568. https://doi.org/10.1021/acs.jpca.1c08717
[42] O. Egorov, M. Rey, A.V. Nikitin, D. Viglaska, *J. Phys. Chem. A* **2022**, *126*, 6429. https://doi.org/10.1021/acs.jpca.2c04822
[43] O. Egorov, M. Rey, R. V. Kochanov, A. V. Nikitin, V. Tyuterev, *Chem. Phys. Lett.* **2023**, *811*, 140216. https://doi.org/10.1016/j.cplett.2022.140216
[44] G. Herzberg, J. Shoosmith, *Nature* **1959**, *183*, 1801. https://doi.org/10.1038/1831801a0
[45] G. Herzberg, *Proc. R. Soc. London A* **1961**, *262*, 291. https://doi.org/10.1098/rspa.1961.0120
[46] G. Herzberg, J. W. C. Johns, *Proc. R. Soc. London A* **1966**, *295*, 107. https://doi.org/10.1098/rspa.1966.0229
[47] R. A. Bernheim, H. W. Bernard, P. S. Wang, L. S. Wood, P. S. Skell, *J. Chem. Phys*. **1970**, *53*, 1280. https://doi.org/10.1063/1.1674129
[48] R. A. Bernheim, H. W. Bernard, P. S. Wang, L. S. Wood, P. S. Skell, *J. Chem. Phys*. **1971**, *54*, 3223. https://doi.org/10.1063/1.1675313
[49] E. Wasserman, W.A. Yager, V.J. Kuck, *Chem. Phys. Lett.* **1970**, *7*, 409. https://doi.org/10.1016/0009-2614(70)80320-7
[50] E. Wasserman, V. J. Kuck, R. S. Hutton, W. A. Yager, *J. Am. Chem. Soc.* **1970**, *92*, 7491. https://doi.org/10.1021/ja00728a054
[51] E. Wasserman, V. J. Kuck, R. S. Hutton, E. D. Anderson, W. A. Yager, *J. Chem. Phys*. **1971**, *54*, 4120. https://doi.org/10.1063/1.1675475
[52] E. Wasserman, R. S. Hutton, V. J. Kuck, W. A. Yager, *J. Chem. Phys*. **1971**, *55*, 2593. https://doi.org/10.1063/1.1676452
[53] J. F. Harrison, L. C. Allen, *J. Am. Chem. Soc.* **1969**, *91*, 807. https://doi.org/10.1021/ja01032a004
[54] J. F. Harrison, *Acc. Chem. Res.* **7,** 378 (1974) https://doi.org/10.1021/ar50083a003
[55] C. F. Bender, H. F. Schaefer III, *J. Am. Chem. Soc.* **1970**, *92*, 4984. https://doi.org/10.1021/ja00719a039
[56] C. F. Bender, H. F. Schaefer III, D. R. Franceschetti, L. C. Allen, *J. Am. Chem. Soc.* **1972**, *94*, 6888. https://doi.org/10.1021/ja00775a004
[57] D. R. McLaughlin, C. F. Bender, H. F. Schaefer III, *Theoret. Chim. Acta* **1972**, *25*, 352. https://doi.org/10.1007/BF00526567
[58] S. V. O'Neil, H. F. Schaefer III, C. F. Bender, *J. Chem. Phys*. **1971**, *55*, 162. https://doi.org/10.1063/1.1675503
[59] P. J. Hay, W. J. Hunt, W. A. Goddard III, *Chem. Phys. Lett.* **1972**, *13*, 30. https://doi.org/10.1016/0009-2614(72)80035-6
[60] G. Herzberg, J. W. C. Johns, *J. Chem. Phys*. **1971**, *54*, 2276. https://doi.org/10.1063/1.1675164
[61] J. A. Mucha, K. M. Evenson, D. A. Jennings, G. B. Ellison, C. J. Howard, *Chem. Phys. Lett.* **1979**, *66*, 244. https://doi.org/10.1016/0009-2614(79)85007-1
[62] T. J. Sears, P. R. Bunker, A. R. W. McKellar, *J. Chem. Phys*. **1981**, *75*, 4731. https://doi.org/10.1063/1.442592
[63] T. J. Sears, P. R. Bunker, A. R. W. McKellar, *J. Chem. Phys*. **1982**, *77*, 5363. https://doi.org/10.1063/1.443784
[64] T. J. Sears, P. R. Bunker, A. R. W. McKellar, K. M. Evenson, D. A. Jennings, J. M. Brown, *J. Chem. Phys*. **1982**, *77*, 5348. https://doi.org/10.1063/1.443783
[65] A. R. W. McKellar, P. R. Bunker, T. J. Sears, K. M. Evenson, R. J. Saykally, S. R. Langhoff, *J. Chem. Phys*. **1983**, *79*, 5251. https://doi.org/10.1063/1.445713
[66] A. R. W. McKellar, C. Yamada, E. Hirota, *J. Chem. Phys*. **1983**, *79*, 1220. https://doi.org/10.1063/1.445926
[67] M. D. Marshall, A. R. W. McKellar, *J. Chem. Phys*. **1986**, *85*, 3716. https://doi.org/10.1063/1.450943
[68] T. J. Sears, *J. Chem. Phys*. **1986**, *85*, 3711. https://doi.org/10.1063/1.450942
[69] P. R. Bunker, T. J. Sears, A. R. W. McKellar, K. M. Evenson, F. J. Lovas, *J. Chem. Phys*. **1983**, *79*, 1211. http://dx.doi.org/10.1063/1.445925

[70] K. M. Evenson, T. J. Sears, A. R. W. McKellar, *J. Opt. Soc. America B* **1984**, *1*, 15. https://doi.org/10.1364/JOSAB.1.000015
[71] A. R. W. McKellar, T. J. Sears, *Can. J. Phys. 1983*, *61*, 480. https://doi.org/10.1139/p83-060
[72] V. Staemmler, *Theoret. Chim. Acta* **1973**, *31*, 49. https://doi.org/10.1007/BF00527438
[73] V. Staemmler, *Theoret. Chim. Acta* **1974**, *35*, 309. https://doi.org/10.1007/BF00548481
[74] A.H. Pakiari, N.C. Handy, *Theoret. Chim. Acta* **1975**, *40*, 17. https://doi.org/10.1007/BF00547909
[75] M. J. S. Dewar, R. C. Haddon, W.-K. Li, W. Thiel, P. K. Weiner, *J. Am. Chem. Soc.* **1975**, *97*, 4540. https://doi.org/10.1021/ja00849a015
[76] J. H. Meadows, H. F. Schaefer III, *J. Am. Chem. Soc.* **1976**, *98*, 4383. https://doi.org/10.1021/ja00431a006
[77] L. B. Harding, W. A. Goddard III, *J. Chem. Phys*. **1977**, *67*, 1777. https://doi.org/10.1063/1.435043
[78] L. B. Harding, W. A. Goddard III, *Chem. Phys. Lett.* **1978**, *55*, 217. https://doi.org/10.1016/0009-2614(78)87005-5
[79] C. W. Bauschlicher Jr., I. Shavitt, *J. Am. Chem. Soc.* **1978**, *100*, 739. https://doi.org/10.1021/ja00471a012
[80] S.-K. Shih, S. D. Peyerimhoff, R. J. Buenker, M. Perić, *Chem. Phys. Lett.* **1978**, *55*, 206. https://doi.org/10.1016/0009-2614(78)87003-1
[81] P. Saxe, H. F. Schaefer III, N. C. Handy, *J. Phys. Chem.* **1981**, *85*, 745. https://doi.org/10.1021/j150607a001
[82] P. R. Taylor, *J. Chem. Phys*. **1981**, *74*, 1256. https://doi.org/10.1063/1.441186
[83] H.-J. Werner, E.-A. Reinsch, *J. Chem. Phys*. **1982**, *76*, 3144 https://doi.org/10.1063/1.443357
[84] H. M. Frey, G. J. Kennedy, *J. Chem. Soc., Chem. Commun.* **1975**, 233. https://doi.org/10.1039/C39750000233
[85] F. Lahmani, *J. Phys. Chem.* **1976**, *80*, 2623. https://doi.org/10.1021/j100565a001
[86] P. F. Zittel, G. B. Ellison, S. V ONeil, E. Herbst, W. C. Lineberger, W. P. Reinhardt, *J. Am. Chem. Soc*. **1976**, *98*, 3731. https://doi.org/10.1021/ja00428a070
[87] J.W. Simons, R. Curry, *Chem. Phys. Lett.* **1976**, *38*, 171. https://doi.org/10.1016/0009-2614(76)80283-7
[88] W. L. Hase, P. M. Kelley, *J. Chem. Phys*. **1977**, *66*, 5093 https://doi.org/10.1063/1.433765
[89] H. M. Frey, G. J. Kennedy, *J. Chem. Soc. Faraday Trans.* 1 **1977**, *73*, 164. https://doi.org/10.1039/F19777300164
[90] R. K. Lengel, R. N. Zare, *J. Am. Chem. Soc.* **1978**, *100*, 7495. https://doi.org/10.1021/ja00492a010
[91] D. Feldmann, K. Meier, H. Zacharias, K. H. Welge, *Chem. Phys. Lett.* **1978**, *59*, 171. https://doi.org/10.1016/0009-2614(78)85641-3
[92] P. C. Engelking, R. R. Corderman, J. J. Wendoloski, G. B. Ellison, S. V. ONeil, W. C. Lineberger, *J. Chem. Phys*. **1981**, *74*, 5460. https://doi.org/10.1063/1.440951
[93] C. C. Hayden, D. M. Neumark, K. Shobatake, R. K. Sparks, Y. T. Lee, *J. Chem. Phys*. **1982**, *76*, 3607. https://doi.org/10.1063/1.443397
[94] S. R. Langhoff, E. R. Davidson, *Int. J. Quantum Chem.* **1973**, *7*, 999. https://doi.org/10.1002/qua.560070515
[95] S. R. Langhoff, *J. Chem. Phys*. **1974**, *61*, 3881. https://doi.org/10.1063/1.1681679
[96] S. R. Langhoff, C. W. Kern, Applications of Electronic Structure Theory. Modern Theoretical Chemistry edited by H.F. Schaefer III **1977**, *4*, 381. https://doi.org/10.1007/978-1-4684-8541-7_10
[97] T. J. Sears, P. R. Bunker, *J. Chem. Phys*. **1983**, *79*, 5265. https://doi.org/10.1063/1.445714
[98] P. R. Bunker, T. J. Sears, *J. Chem. Phys*. **1985**, *83*, 4866. https://doi.org/10.1063/1.449747
[99] D. G. Leopold, K. K. Murray, A. E. S. Miller, W. C. Lineberger, *J. Chem. Phys*. **1985**, *83*, 4849. https://doi.org/10.1063/1.449746
[100] L. H. Coudert, B. Gans, F. Holzmeier, J.-C. Loison, G. A. Garcia, C. Alcaraz, A. Lopes, A. Röder, *J. Chem. Phys*. **2018**, *149*, 224304. https://doi.org/10.1063/1.5062834
[101] H. Petek, D. J. Nesbitt, P. R. Ogilby, C. B. Moore, *J. Phys. Chem.* **1983**, *87*, 5367. https://doi.org/10.1021/j150644a012
[102] H. Petek, D. J. Nesbitt, D. C. Darwin, C. B. Moore, *J. Chem. Phys*. **1987**, *86*, 1172. https://doi.org/10.1063/1.452263
[103] H. Petek, D. J. Nesbitt, C. B. Moore, F. W. Birss, D. A. Ramsay, *J. Chem. Phys*. **1987**, *86*, 1189. http://dx.doi.org/10.1063/1.452264
[104] H. Petek, D. J. Nesbitt, D. C. Darwin, P. R. Ogilby, C. B. Moore, D. A. Ramsay, *J. Chem. Phys*. **1989**, *91*, 6566. https://doi.org/10.1063/1.457375

[105] A. R. Hoy, P. R. Bunker, *J. Mol. Spectrosc.* **1974**, *52*, 439. https://doi.org/10.1016/0022-2852(74)90191-X
[106] P. R. Bunker, B. M. Landsberg, *J. Mol. Spectrosc.* **1977**, *67*, 374. https://doi.org/10.1016/0022-2852(77)90048-0
[107] A. R. Hoy, P. R. Bunker, *J. Mol. Spectrosc.* **1979**, *74*, 1. https://doi.org/10.1016/0022-2852(79)90019-5
[108] J. T. Hougen, P. R. Bunker, J. W. C. Johns, *J. Mol. Spectrosc.* **1970**, *34*, 136. https://doi.org/10.1016/0022-2852(70)90080-9
[109] P. Jensen, *Comp. Phys. Rep.* **1983**, *1*, 1. https://doi.org/10.1016/0167-7977(83)90003-5
[110] P. Jensen, P. R. Bunker, *J. Mol. Spectrosc.* **1983**, *99*, 348. https://doi.org/10.1016/0022-2852(83)90319-3
[111] P. Jensen, P. R. Bunker, *J. Mol. Spectrosc.* **1986**, *118*, 18. https://doi.org/10.1016/0022-2852(86)90220-1
[112] A. D. McLean, P. R. Bunker, R. M. Escribano, P. Jensen, *J. Chem. Phys.* **1987**, *87*, 2166. http://dx.doi.org/10.1063/1.453141
[113] D. C. Comeau, I. Shavitt, P. Jensen, P. R. Bunker, *J. Chem. Phys.* **1989**, *90*, 6491. https://doi.org/10.1063/1.456315
[114] I. N. Kozin, P. Jensen, *J. Mol. Spectrosc.* **1997**, *183*, 398. https://doi.org/10.1006/jmsp.1997.7288
[115] A. Tajti, P. G. Szalay, A. G. Császár, M. Kállay, J. Gauss, E. F. Valeev, B. A. Flowers, J. Vázquez, J. F. Stanton, *J. Chem. Phys.* **2004**, *121*, 11599. http://dx.doi.org/10.1063/1.1811608
[116] D. M. Medvedev, L. B. Harding, S. K. Gray, *Mol. Phys.* **2006**, *104*, 73. http://dx.doi.org/10.1080/00268970500238663
[117] H. Ozeki, S. Saito, *The Astrophysical Journal* **1995**, *451*, L97. https://doi.org/10.1086/309696
[118] H. Ozeki, S. Saito, *J. Chem. Phys.* **1996**, *104*, 2167. https://doi.org/10.1063/1.470972
[119] J. Nolte, F. Temps, H. Gg. Wagner, M. Wolf, T. J. Sears, *J. Chem. Phys.* **1994**, *100*, 8706. http://dx.doi.org/10.1063/1.466726
[120] H. Ozeki, S. Bailleux, G. Wlodarczak, *A&A* **2011**, *527*, A64. https://doi.org/10.1051/0004-6361/201016043
[121] P. J. Knowles, C. Hampel, H.-J. Werner, *J. Chem. Phys.* **1993**, *99*, 5219. http://dx.doi.org/10.1063/1.465990
[122] P. J. Knowles, C. Hampel, H.-J. Werner, *J. Chem. Phys.* **2000**, *112*, 3106. http://dx.doi.org/10.1063/1.480886
[123] T. J. Lee, P. R. Taylor, *Int. J. Quant. Chem.* **1989**, *36*, 199. https://doi.org/10.1002/qua.560360824
[124] C. L. Janssen, I. M. B. Nielsen, *Chem. Phys. Lett.* **1998**, *290*, 423. https://doi.org/10.1016/S0009-2614(98)00504-1
[125] G. Duxbury, Ch. Jungen, *Mol. Phys.* **1988**, *63*, 981. https://doi.org/10.1080/00268978800100721
[126] A. Alijah, G. Duxbury, *Mol. Phys.* **1990**, *70*, 605. https://doi.org/10.1080/00268979000102621
[127] W. H. Green, N. C. Handy, P. J. Knowles, S. Carter, *J. Chem. Phys.* **1991**, *94*, 118. https://doi.org/10.1063/1.460385
[128] W. Xie, C. Harkin, H. -L. Dai, *J. Chem. Phys.* **1990**, *93*, 4615. http://dx.doi.org/10.1063/1.458701
[129] G. V. Hartland, D. Qin, H.-L. Dai, *J. Chem. Phys.* **1995**, *102*, 6641. https://doi.org/10.1063/1.469136
[130] J. -P. Gu, G. Hirsch, R. J. Buenker, M. Brumm, G. Osmann, P. R. Bunker, P. Jensen, *J. Mol. Spectrosc.* **2000**, *517–518*, 247. https://doi.org/10.1016/S0022-2860(99)00256-2
[131] T. H. Dunning, *J. Chem. Phys.* **1989**, *90*, 1007. https://doi.org/10.1063/1.456153
[132] K. A. Peterson, D. E. Woon, T. H. Dunning, *J. Chem. Phys.* **1994**, *100*, 7410. https://doi.org/10.1063/1.466884
[133] G. Knizia, T. B. Adler, H.-J. Werner, *J. Chem. Phys.* **2009**, *130*, 054104. https://doi.org/10.1063/1.3054300
[134] J. Gauss, A. Tajti, M. Kállay, J. F. Stanton, P. G. Szalay, *J. Chem. Phys.* **2006**, *125*, 144111. https://doi.org/10.1063/1.2356465
[135] A.D. Boese, M. Oren, O. Atasoylu, M.L. Jan Martin, M. Kállay, J. Gauss, *J. Chem. Phys.* **2004**, *120*, 4129. https://doi.org/10.1063/1.1638736
[136] D. Viglaska, M. Rey, A. V. Nikitin, V. G. Tyuterev, *J. Chem. Phys.* **2020**, *153*, 084102. https://doi.org/10.1063/5.0016365
[137] W. Kutzelnigg, *Mol. Phys.* **2007**, *105*, 2627. http://dx.doi.org/10.1080/00268970701604671
[138] J. Tennyson, M. A. Kostin, P. Barletta, G. J. Harris, O. L. Polyansky, J. Ramanlal, N. F. Zobov, *Comp. Phys. Comm.* **2004**, *163*, 85. https://doi.org/10.1016/j.cpc.2003.10.003

[139] V. Szalay, *J. Mol. Spectrosc.* **1988**, *128*, 24. https://doi.org/10.1016/0022-2852(88)90204-4
[140] V. Szalay, *J. Chem. Phys*. **1990**, *92*, 3633. https://doi.org/10.1063/1.457819
[141] G. Tarczay, A. G. Császár, W. Klopper, V. Szalay, W. D. Allen, H. F. Schaefer III, *J. Chem. Phys.* **1999**, *110*, 11971. http://dx.doi.org/10.1063/1.479135
[142] I. E. Gordon, L. S. Rothman, R. J. Hargreaves, R. Hashemi, E. V. Karlovets, F. M. Skinner, E. K. Conway, C. Hill, R. V. Kochanov, Y. Tan, P. Wcisłof, A. A. Finenko, K. Nelson, P. F. Bernath, M. Birk, V. Boudon, A. Campargue, K. V. Chance, A. Coustenis, B. J. Drouinm, J.-M. Flaud, R. R. Gamache, J. T. Hodges, D. Jacquemart, E. J. Mlawer, A. V. Nikitin, V. I. Perevalov, M. Rotger, J. Tennyson, G. C. Toon, H. Tran, V. G. Tyuterev, E. M. Adkins, A. Baker, A. Barbe, E. Canè, A. G. Császár, O. Egorov, A. J. Fleisher, H. Fleurbaey, A. Foltynowicz, T. Furtenbacher, J. J. Harrison, J.-M. Hartmann, V.-M. Horneman, X. Huang, T. Karman, J. Karns, S. Kassi, I. Kleiner, V. Kofman, F. Kwabia-Tchana, T. J. Lee, D. A. Long, A. A. Lukashevskaya, O. M. Lyulin, V. Yu. Makhnev, W. Matt, S. T. Massie, M. Melosso, S. N. Mikhailenko, D. Mondelain, H. S. P. Müller, O. V. Naumenko, A. Perrin, O.L. Polyansky, E. Raddaoui, P. L. Raston, Z. D. Reed, M. Rey, C. Richard, R. Tóbiás, I. Sadiek, D. W. Schwenke, E. Starikova, K. Sung, F. Tamassia, S. A. Tashkun, J. Vander Auwera, I. A. Vasilenko, A. A. Vigasin, G. L. Villanueva, B. Vispoel, G. Wagner, A. Yachmenev, and S. N. Yurchenko, *J. Quant. Spectrosc. Radiat. Transfer* **2022**, *277*, 107949. https://doi.org/10.1016/j.jqsrt.2021.107949
[143] T. Delahaye, R. Armante, A. Chédin, L. Crépeau, C. Crevoisier, V. Douet, N. Jacquinet-Husson, A. Perrin, N. A. Scott, A. Barbe, V. Boudon, A. Campargue, L. H. Coudert, V. Ebert, J.-M. Flaud, R. R. Gamache, D. Jacquemart, A. Jolly, F. Kwabia Tchana, A. Kyuberis, G. Li, O. M. Lyulin, L. Manceron, S. Mikhailenko, N. Moazzen-Ahmadi, H. S. P. Müller, O. V. Naumenko, A. Nikitin, V. I. Perevalov, C. Richard, E. Starikova, S. A. Tashkun, Vl. G. Tyuterev, J. Vander Auwera, B. Vispoel, A. Yachmenev, and S. Yurchenko, *J. Mol. Spectrosc.* **2021**, *380*, 111510. https://doi.org/10.1016/j.jms.2021.111510
[144] M. Rey, *J. Chem. Phys*. **2022**, *156*, 224103. https://doi.org/10.1063/5.0089097
[145] H. M. Pickett, *J. Mol. Spectrosc.* **1991**, *148*, 371. https://doi.org/10.1016/0022-2852(91)90393-O
[146] A. V. Burenin, T. M. Fevral'skikh, E. N. Karyakin, O. L. Polyansky, S. M. Shapin, *J. Mol. Spectrosc.* **1983**, *100*, 182. https://doi.org/10.1016/0022-2852(83)90035-8
[147] O. L. Polyansky, *J. Mol. Spectrosc.* **1985**, *112*, 79. https://doi.org/10.1016/0022-2852(85)90193-6
[148] S. P. Belov, I. N. Kozin, O. L. Polyansky, M. Yu. Tret'yakov, N. F. Zobov, *J. Mol. Spectrosc*. **1987**, *126*, 113. https://doi.org/10.1016/0022-2852(87)90081-6
[149] H. M. Pickett, J. C. Pearson, C. E. Miller, *J. Mol. Spectrosc.* **2005**, *233*, 174. https://doi.org/10.1016/j.jms.2005.06.013
[150] Vl. G. Tyuterev, *J. Mol. Spectrosc.* **1992**, *151*, 97. https://doi.org/10.1016/0022-2852(92)90009-D
[151] V. I. Starikov, S. A. Tashkun, Vl. G. Tyuterev, *J. Mol. Spectrosc.* **1992**, *151*, 130. https://doi.org/10.1016/0022-2852(92)90010-L
[152] V. I. Starikov, S. N. Mikhailenko, *J. Phys. B: At. Mol. Opt. Phys.* **2000**, *33*, 2141. https://doi.org/0.1088/0953-4075/33/11/314